

## Once upon a Time in Italy: The Tale of the Morandi Bridge

Gian Michele Calvi, Matteo Moratti, Gerard J. O'Reilly, Nicola Scattarreggia, Ricardo Monteiro, Daniele Malomo, Paolo Martino Calvi & Rui Pinho

To cite this article: Gian Michele Calvi, Matteo Moratti, Gerard J. O'Reilly, Nicola Scattarreggia, Ricardo Monteiro, Daniele Malomo, Paolo Martino Calvi & Rui Pinho (2018): Once upon a Time in Italy: The Tale of the Morandi Bridge, Structural Engineering International, DOI: [10.1080/10168664.2018.1558033](https://doi.org/10.1080/10168664.2018.1558033)

To link to this article: <https://doi.org/10.1080/10168664.2018.1558033>



Published online: 20 Dec 2018.



Submit your article to this journal [↗](#)









Article views: 30



View Crossmark data [↗](#)

# Once upon a Time in Italy: The Tale of the Morandi Bridge

Gian Michele Calvi , Eucentre Foundation, Pavia, Italy; Matteo Moratti, Studio Calvi Ltd, Pavia, Italy; Gerard J. O'Reilly , IUSS, Pavia, Italy; Nicola Scattarreggia , IUSS, Pavia, Italy; Ricardo Monteiro , IUSS, Pavia, Italy; Daniele Malomo , Mosayk Ltd, Pavia, Italy; Paolo Martino Calvi, University of Washington, Seattle, USA; Rui Pinho , University of Pavia, Italy. Contact: gm.calvi@eucentre.it  
DOI: 10.1080/10168664.2018.1558033

## Abstract

On 14 August 2018 at 11:35 AM, a relevant portion (about 243 m) of the viaduct over the Polcevera river in Genoa collapsed, killing 43 people. The bridge was designed in the early 1960s by Riccardo Morandi, a well-known Italian engineer, and opened to the public in 1967. The collapsed part of the bridge essentially comprised an individual self-standing structure spanning 171 m and two simply-supported connecting Gerber beam systems, each spanning 36 m from the self-standing structure to the adjacent portions of the bridge. This paper aims to reminisce the complete story of the bridge, from the Italian construction boom in the 1960s to some of the issues that soon arose thereafter: the strengthening intervention in the 1990s, the subsequent structural monitoring and, finally, the strengthening project never brought to fruition. Potential reasons for the collapse are discussed, together with some of the possible inadequacies of the bridge, its maintenance and loading history based on critical reflection, comparison with specific features of bridge construction practice today and results obtained using numerical models with different levels of refinement. Since the entire matter (specifically the debris) was considered classified by the investigating magistrate in the immediate aftermath of the bridge collapse, this work is based entirely on publicly available material.

**Keywords:** Morandi Bridge; structural collapse; forensic engineering; AEM modelling

## Introduction

### *Construction of Road Infrastructure in the 1960s*

It is commonly stated, and easy to verify, that the 1960s were an extraordinary time for the construction of freeways. The era of great bridge construction had started much earlier, as masterfully described by Petrovsky<sup>1</sup> with main reference to the US, but bridges were perceived as standalone masterpieces to cross rivers or straits, rather than part of a roadway system. It was on 29 June 1956 that President Eisenhower signed the Federal-Aid Highway Act in the US, initiating the “Greatest Decade”,<sup>2,3</sup> or the construction of the Interstate System that originally included around 60 000 km of roadways. When the Eisenhower administration ended in January 1961, about one fourth of this system had been opened to traffic. With an average construction of about 5000 km per year, President Eisenhower’s successor, President Kennedy, refused to follow the suggestions of

cutting back the programme and opposed the reduction of a temporary USD\$0.01 gas tax per gallon ( $\approx$  3.8 litres) established to fund the Interstate Program. By the end of 1966, some 29 000 km of highways had been completed, with a total cost of about \$25 billion. According to a document submitted to the US Congress in 1965,<sup>3</sup> the complete system (which required additional funding estimated to be about \$20 billion) would have included “12,957 interchanges requiring 22,252 individual structures, as well as 20,748 other highway grade-separation structures, 4,361 railroad grade separations, and 14,806 other bridges and tunnels”.

In Europe, the construction of freeways started much earlier with the initial but limited experience in Italy in the 1920s and a massive programme in Germany in the late 1930s, where some 4000 km of roads were built between 1935 and 1940, which inspired President Eisenhower to say: “Germany had made me see the wisdom of broader ribbons across the land”.<sup>2</sup> However, it was after

the Second World War and mainly in the 1960s that most European countries constructed the backbone of the modern freeway system. In Italy, the 760 km “*Autostrada del Sole*” freeway system linking Milan to Rome and Naples was designed and built between 1956 and 1964, coinciding with the American “greatest decade”. Regardless of its relatively small length, this freeway represented an achievement of sorts, due to the ingenuity required for its conception and construction, as a result of the challenging topography of the Italian territory, particularly in the mountainous area between Bologna and Florence. Indeed, a total of 853 bridges and viaducts (without considering 572 overpasses) and 38 tunnels needed to be constructed.

There is little need for any detailed analysis to state that a significant fraction of both North American and European infrastructure has reached or is reaching its nominal design life, requiring the allocation of relevant resources for their assessment, repair and upgrading. In particular, entire inventories of structures are in need of assessment to allow rational prioritisation in the allocation of limited resources available. This implies the issue of rapid assessment methods to perform an initial screening, followed by the application of more refined approaches (with a proportional acquisition of more data) to a limited number of cases and possibly the implementation of effective and well-focused monitoring systems in specific situations. The collapse of the bridge in Genoa has attracted media attention worldwide, with *The New York Times*<sup>4</sup> recently summarising that:

- in France, the highway system comprising 12 000 bridges is in a state of chronic underinvestment, with 7% having damage that could eventually result in collapse if not addressed;
- in Germany, of the 39 621 bridges monitored by the Federal Government, 10.6% are in a condition that

is not satisfactory and 1.8% are in “inadequate” condition;

to name but a few, with similar examples reported for other European countries.

### ***Design of Bridges and Pre-stressed Structures in Italy in the 1960s***

In the aftermath of the Second World War, bridge design was essentially retracing the experiences of the 1930s and the dominant structural system was probably still the arch.<sup>5</sup> Concrete arch bridges had recurrent spans in the range of 60–80 m and even in the construction of the *Autostrada del Sole*, a span of 100 m was regarded as a limit for standard practice. Traffic loads were not significantly smaller with respect to those considered today, with the exception of the maximum uniformly distributed load, which was set at 4 kN/m<sup>2</sup>, against the 6 kN/m<sup>2</sup> typically adopted nowadays. Cable-stayed bridges were seldom considered, probably because of the circular problem of absorbing the axial force component in the deck that tended to increase its cross-section size, which in turn would imply a higher self-weight, and hence increase the axial force. The advent of light composite deck sections that would allow long span cable-stayed bridges was still a few decades away. Pre-stressed concrete had been conceived and experimented starting in the late twenties, mainly by Freyssinet, but even enthusiastic and brilliant researchers and engineers, like Torroja in Spain, Dischinger in Germany and Colonnetti in Italy, faced a then hardly surmountable obstacle in the difficulty of producing high strength steel, proven to be a fundamental prerequisite for its practical implementation.

After the Second World War, things changed at an impressive pace, particularly in Italy. While it is hard to find pre-stressed concrete even mentioned in the standard text book used at the Politecnico di Milano to teach bridge design in the 1950s,<sup>6</sup> between 1945 and 1960 a number of design manuals were published and a number of patents were imported or deposited on elastic coaction, cable anchoring, etc. Pre-stressed concrete technology would have still been regarded as being in its infancy but nevertheless, gifted designers like Levi, Cestelli-Guidi, Pizzetti, Oberti and Zorzi immediately began applying it to relatively long span bridges.<sup>7</sup> Solutions to

problems related to creep, temperature variations, strand relaxation, redistribution effects in statically indeterminate structures, nonlinear and ultimate response, were only intuitively considered, and sometimes simply neglected. It was only years later, with the development of dedicated software, that it became possible to model most of such complex time-dependent effects.

In the context briefly depicted above, Riccardo Morandi was a very unique individual and the bridge over the Polcevera river in Genoa was a very unique design case, reflecting each other. The bridge was cable-stayed with single post-tensioned concrete stays and spans exceeding 200 m. The deck was temporarily pre-stressed during construction and locally post-tensioned in its final configuration. The connecting simply supported spans were made of 36 m precast pre-stressed Gerber beams. It is evident that the definition of “cable-stayed bridge” refers today to quite different structural configurations,<sup>8</sup> with a large number of stays used also as progressive supports for the deck, to be kept as light as possible. The single concrete stays used in the so-called “Morandi bridge” did not garner much popularity in the following decades, with essentially no followers. All in all, however, it was an absolute masterpiece but also a daring combination of advanced and relatively new technology assembled in a clear and relatively simple structural scheme. Nevertheless, as would be unveiled in the subsequent years, it possessed a high potential for issues raising from some of the features mentioned above.

### ***Earthquakes and Disasters in the 1960s***

It may be surprising to realise that not much attention was paid to potential extreme actions on bridges, such as those generated by seismic loading, even though the 1960s were not a peaceful time from the point of view of ground shaking:

- On 22 May 1960, the Great Chilean earthquake hit a region some 570 km south of Santiago. With a magnitude of 9.5, this is to date the largest energy ever released by a recorded event. The subsequent tsunami generated waves up to 25 metres on the Chilean coast and

raced across the Pacific Ocean devastating Hawaii, Japan and the Philippines.

- On 26 July 1963, a much smaller earthquake (M<sub>w</sub> = 6.1) hit Skopje in Macedonia inducing more than 1000 victims and leaving more than 200 000 people homeless. About 8.5% of the buildings were destroyed, 34% had to be demolished and 36% required major repairs,<sup>9</sup> whereas the 15th century stone bridge over the river Vardar was not reported to have suffered major damage. In the aftermath, a school building was base isolated using rubber bearings, for the first time in the world.<sup>10</sup>
- On 27 March 1964, a M<sub>w</sub> = 9.2 (the largest ever recorded in North America) earthquake occurred in Alaska, not far from Anchorage. Permanent ground displacements in the range of 9 m were recorded. The Seward Highway was devastated and severe damage to bridges was reported, such as the span of the Million Dollar Bridge that slipped off its pier due to soil liquefaction.<sup>11</sup>

In Italy, one of the most tragic catastrophes was the Vajont dam disaster in 1963. A relevant portion of the mountain Toc (about 260 million cubic metres) slid into the reservoir, causing a flood wave that killed approximately 2000 people in the towns further down the valley. The 262 m tall concrete dam remained essentially undamaged, inspiring discussions about an *engineering masterpiece built in the wrong place*.<sup>12</sup>

It is even more surprising to learn that seismic assessment of most bridges built in absence of any seismic design code (in Italy the first one was released in 2003, with the OPCM 3274<sup>13</sup> has not been performed to date, at least not in regions of relatively modest seismic hazard. Likewise, such an assessment has also not been carried out even in outstanding cases like the one considered in this study, which exposure, in terms of consequences of traffic interruption or collapse, is extremely high. The OPCM 3274<sup>13</sup> did indeed foresee a compulsory verification of the seismic safety of infrastructures *which functionality was fundamental for the purpose of civil protection or for which collapse would imply relevant consequences*, but in the (fifteen) years subsequent to its release, measures and provisions have not

been effective in providing specific time constraints for assessment and possible strengthening.

### Bridge Collapses

Bridge collapses are reported all over history and this is not the place for a recapitulation on the subject. It is, however, of interest to note that failures can be attributed to three main categories:

- (a) Unexpected external actions, possibly due to both natural or anthropogenic catastrophes (e.g. earthquakes, floods or sudden impacts);
- (b) Deterioration of mechanical properties, possibly due to corrosion of the reinforcement or concrete carbonation or fatigue, sometimes also in conjunction with increased traffic load (as in the case of fatigue);
- (c) Inadequate original design or construction, possibly related to unknown structural effects, sometimes related to dynamic actions.

A dramatic and well-known example of type c) is the Tacoma Narrows Bridge that collapsed soon after completion in 1940.<sup>1</sup> The advisory engineer to the bond purchaser, Theodore Condon, expressed concerns about its horizontal slenderness (1:72, much smaller than those of all existing suspension bridges; that of the conceptually similar Golden Gate Bridge, completed three years earlier and featuring a much longer central span (4200 versus 2800 ft), was about 1:47). The reputation and the self-confidence of the main designer, Leon Moisseff, prevailed against what were then deemed unjustified qualms and the bridge collapsed four months after completion, when facing a wind of about 40 knots. The explanation was found by von Kármán, who describes its experiment with a van and a model of the bridge in his magniloquent autobiography.<sup>14</sup> As reported by Petrovsky<sup>1</sup> “The

villain was the Kármán vortices, named after the investigator himself, or the whirlpool of air that were shed in the wake behind the moving model and thus buffeted it”.

Recent reinforced concrete bridge collapses seem to be often related to shear problems or loss of post-tensioning, essentially ascribable to category b) above, and more rarely to c). Examples of such cases include<sup>15</sup>:

- (1) The Laval overpass in Quebec, Canada, which failed in shear killing five in 2006.<sup>16</sup> The Laval collapse led to an extensive review of 135 bridge structures in Quebec, resulting in 28 bridges being demolished and further 25 being repaired immediately.<sup>17</sup>
- (2) A highway overpass that failed on 29 October 2016 in Lecco, Italy, killing one and injuring five.<sup>18–20</sup> The bridge was a concrete structure with a drop-in-span that, from publicly available videos, appears to have suffered a brittle failure near the drop-in span support ledge; the detailed investigation of the probable causes of collapse is currently ongoing.
- (3) A post-tensioned viaduct near Fossano, Italy, on 19 April 2017. Two police officers reported having been underneath the bridge as it began to collapse. The collapsing bridge span fell on and destroyed the officers’ vehicle; however, since the failure reportedly occurred over several seconds, the officers were able to escape unharmed.<sup>20</sup>
- (4) The bridge “Santo Stefano”, near Messina, which collapsed on 23 April 1999. This case is less known, possibly because no casualties were involved, but deserves to be mentioned here because it had been designed by Morandi and the deck (with span 78 m and a box section) was post-tensioned with the same system employed in the Genoa bridge.<sup>21</sup>

Considering the above (i.e. that type b) collapses of reinforced concrete bridges have been predominant in the past, it is no surprise that in the case of the Morandi bridge, media and public opinion immediately focused on maintenance and deterioration. However, it is important to also explore whether the bridge was flawed by some “original sin”, not with the aim of establishing and assigning fault or blame, but rather to examine possible reasons for the Morandi bridge collapse using robust engineering rationale.

## The Morandi Bridge: Design and Construction

### Description of the Bridge

The design and construction of the bridge is described in detail by Morandi himself in a long paper published in 1967<sup>22</sup> and in an unpublished report.<sup>23</sup> Whilst those documents refer to the entire bridge structure (Fig. 1), the attention here will focus on the three “balanced systems”, shown in Fig. 2, that constitute the large span portions of the viaduct. Each of the 12 support points of the bridge was numbered sequentially from the Savona side shown in Fig. 1, with piers 9, 10 and 11 comprising the aforementioned balanced systems. It was pier number 9 that collapsed on 14 August 2018. Above the foundation, which is not discussed here, each balanced system comprises the following main elements:

- a) A pier with eight inclined struts (with cross-section varying between  $4.5 \times 1.2$ – $2.0 \times 1.2$  m) that props the deck over a distance of about 42 m.
- b) An antenna with two A-shaped structures (element cross-section varying between  $4.5 \times 0.9$ – $2.0 \times 3.0$  m) that converge about 45 m above the deck level.
- c) A main deck with a five-sector box section of depth variable between 4.5 and 1.8 m, an upper and lower

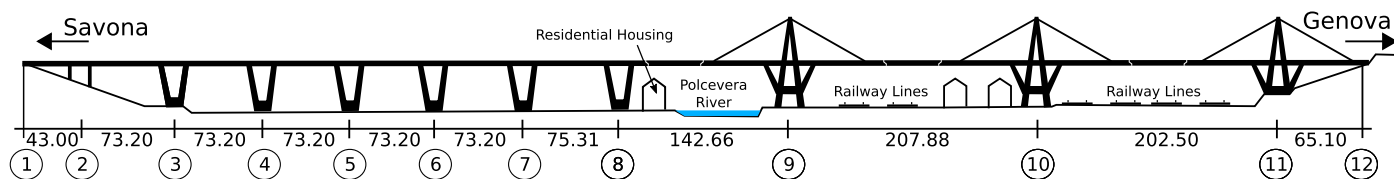


Fig.1: Schematic of the piers and distances between each support of the Morandi Bridge, with the three balanced systems shown to pass over residential areas, numerous transportation lines and the Polcevera river (although not shown, the area between piers 1 and 8 is also heavily industrialised) (Units: m)

slab 160 mm thick, and six deep webs with thickness varying between 180 and 300 mm. In its final configuration, the deck of the *balanced system* 9 was 172 m long and supported at four locations: two of these from underneath the deck, provided by the pier inclined struts at the aforementioned spacing of 42 m, and the other two from above, provided by the cable stays at a distance of 152 m. There was therefore no connection between the deck and the antenna. Two 10 m cantilevers completed the deck length.

- d) Four *transverse link girders*, connecting stays and pier trusses to the deck.
- e) Four *cable stays*, hanging from the antenna's top and intersecting the deck at an angle of about 30°.
- f) Two *simply-supported Gerber beam spans* connecting the balanced system to the adjacent

parts of the bridge. Each Gerber supported span was 36 m long and comprised six precast prestressed beams, with a variable depth equal to 2.20 m at mid span, sitting on Gerber saddles protruding from the main deck.

### Construction Process

Whilst the construction of the pier and antenna is reported to have followed traditional methods (this is also evident from the photos taken during the construction), the completion of the main deck was inspired by a rather original and ingenious expedient. Indeed, the deck was erected through a segmental construction process departing from each side of the antenna centreline, and each segment (of a maximum length of 5.5 m, which was the capacity of the launching girder) was temporarily connected to the previously constructed

portion of the structure by means of post-tensioned cables laying on top of the deck and slightly inclined by means of steel supports (2.1 m tall) located in correspondence with the inclined struts of the pier.

Following the progressive connection and post-tensioning of the stays, the temporary cables were progressively removed, finally obtaining a five-span continuous deck compressed by the horizontal component of the cable stays' force in the three central spans. According to the designer words "at this stage the deck is essentially lacking any longitudinal reinforcement, with the exception of the end cantilever parts and of the areas next to the intermediate supports".<sup>22</sup> The conclusive construction operation was termed the "homogenisation of the system" by Morandi and described as the casting of concrete shells around the steel cable stays, their post-

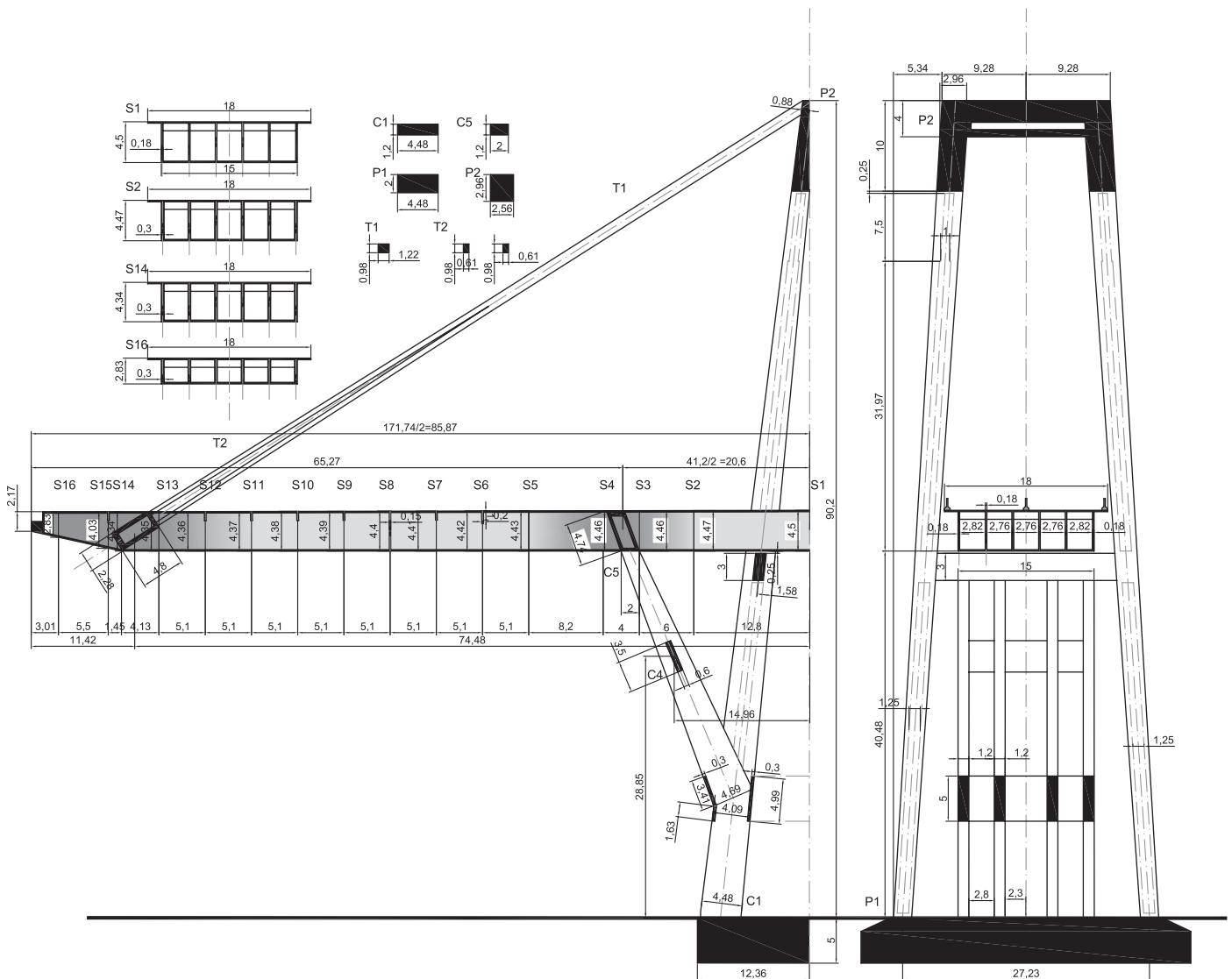


Fig. 2: Longitudinal and transversal section of one of the "balanced systems" that constituted the large span portions of the viaduct (Units: m)

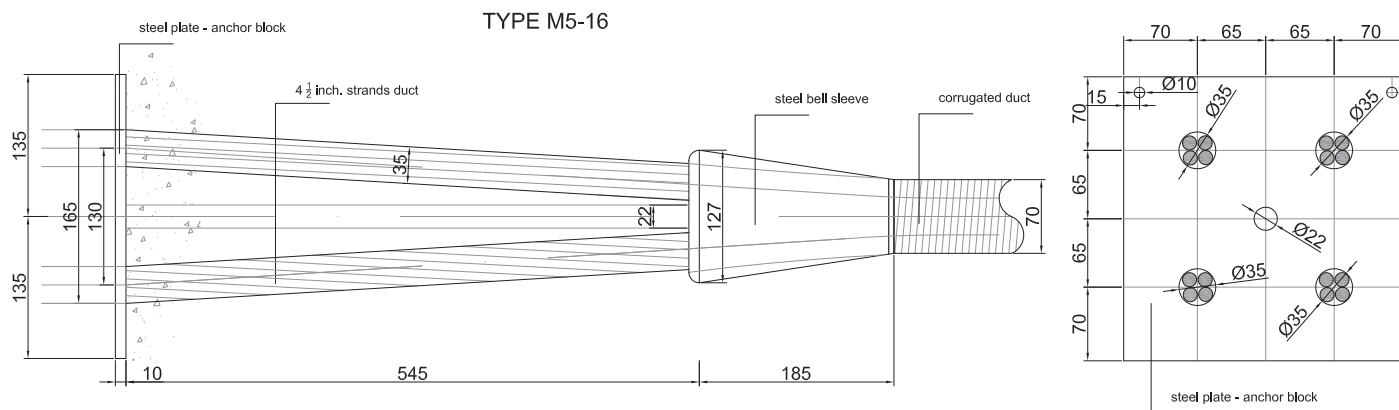


Fig. 3: Details of the end part of a 16 1/2 inch strands post-tensioning cable according to the Morandi System,<sup>24</sup> re-drawn (Units: mm)

compression, while still not bonded to the stays, and the final “usual injection” of all ducts with the definitive connection between cable stays and deck.<sup>22</sup>

The deck extremities were deformed upwards by appropriately tensioning the cable stays, to obtain a straight

configuration upon mounting the 36 m simply supported Gerber beams and completing the dead weight on the entire deck. It is evident from description and construction photos that this phase followed the casting of the concrete stays and the cable injection. According to Morandi, in its final configuration the bridge would have

responded elastically to any action (traffic, temperature and wind, whereas no mention is made to earthquakes). In addition, the stays concrete would have always been in compression (therefore not susceptible to cracking and consequent corrosion potential) and stiffer (thus less sensitive to fatigue problems and less

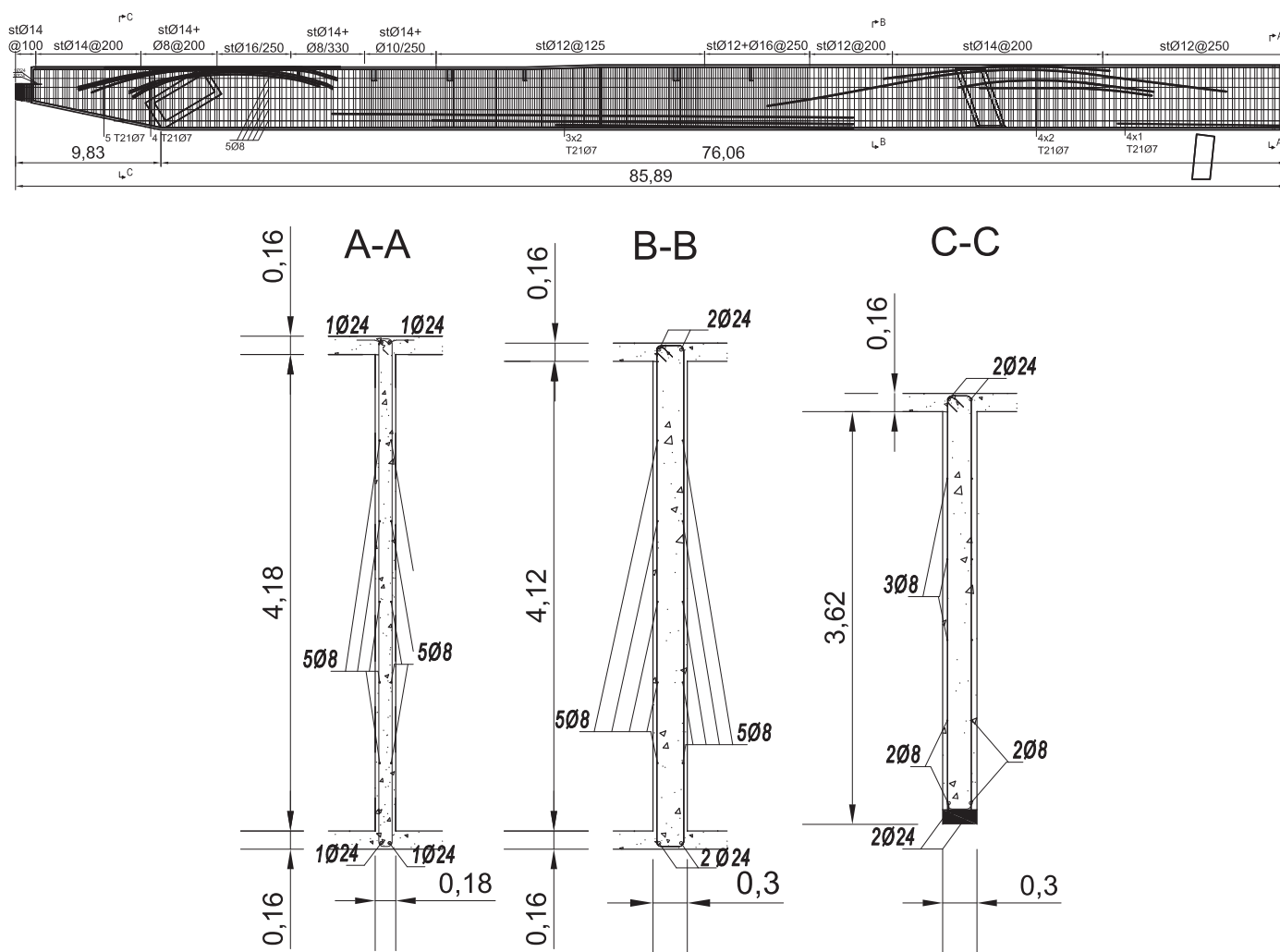


Fig. 4: Geometry and reinforcement (top) in addition to three cross-sections (bottom) of the main deck (Units: m)

prone to deck rotation and to horizontal displacement of the antenna tip).

### The Morandi Pre-compression System

Morandi developed and patented a pre-compression system ( $M_5$ , described in detail in<sup>24</sup> based on seven-wire strands with the following characteristics:

Nominal diameter	12.7 mm (½ inch)
Nominal section	92.90 mm <sup>2</sup>
Minimum strength	163 kN (i.e. 1758 MPa)
Minimum elongation capacity	3.5 % (measured on a base of 610 mm)

He recommended a working stress of 1000 MPa and an initial stress of 1200 or 1300 MPa. In all cases, the strands were coupled in groups of four; an example is the end part of  $M_5/16$ , depicted in Fig. 3—each of the four terminal ducts and plate holes contains four strands. Comparing the Morandi  $M_5$  system to modern practice (e.g. Ref. [25]) it is striking how tight the strands were located inside the duct. In modern practice, the void section left for duct injection is around 50% larger than in the Morandi case, though varying with the number of strands. This is even more surprising considering that today's injection materials are far more fluid than those used some sixty years ago, meaning their penetration into the duct is much easier. It may be thus concluded that the ducts used in the case of the Morandi bridge were essentially impossible to be injected and it is thus difficult to understand the meaning of “the usual injection of cement mortar will be executed”.<sup>23</sup>

From some descriptions and photos reproduced in the report of the *Commission of the Ministry of Infrastructures and Transportation*,<sup>26</sup> no cement mortar injection appears visible. This is consistent with the considerations above and may shed some light on behaviour potentially different from the one that was expected in terms of corrosion protection, effects of fatigue, structural stiffness and localised sectional response.

### Pier and Antenna

The high vertical force, combined with the “balancing” of the system and the relatively low live loads with respect to self-weight and dead load (less than 20%, with reference to the deck only), rendered pier and antenna elements as members essentially compressed. As a consequence, there was no need for reinforcement to absorb tensile forces and, consistently with his vision, Morandi used a minimum reinforcement level. In general, this minimum seems to be set in the range of 0.3% of the concrete section. For example, at the base of the antenna, in a section of  $4.5 \times 0.9$  m, the steel reinforcement was 4 Ø30 mm plus 20 Ø24 mm bars, resulting in a geometrical percentage of longitudinal reinforcement of  $\rho_s=0.29\%$ . A combination of smooth (with minimum yield strength  $f_{y,min}=270$  MPa) and deformed ( $f_{y,min}=440$  MPa) rebars was used. At casting interruption sections, the continuity of smooth bars relied on standard hooks only. Horizontal reinforcement was provided by Ø10 mm stirrups at 250 mm spacing. Whilst this reinforcement could give a significant contribution to shear strength, considering the large depth of the section, the concrete was essentially unconfined, according to modern concrete detailing standards.

### Main Deck

The geometry of the deck section has already been briefly described above, with its reinforcement being now herein discussed. Morandi had noted that some parts of the deck were *essentially lacking longitudinal reinforcement*, a statement that seems indeed aligned with the actual reinforcement quantities employed, especially if compared to today's standard practice. From the original drawings, reproduced in Fig. 4, it appears that the continuous reinforcement provided at each beam was 4 Ø24 mm and 10 Ø8 mm bars; on a standard concrete beam section of  $0.18 \times 4.5$  m, a reinforcement percentage of  $\rho_s=0.29\%$  is thus obtained. Further, it appears that 8 pre-compression cables with 21 Ø7 mm wires (total  $A_{sp}=6465$  mm<sup>2</sup>) were located on top of the beam in a region of about 12 m on each side of the connection with the pier inclined strut and in the cantilever

hanging out of the stays connection; these cables do not seem to be related to the aforementioned  $M_5$  patented system, where only ½ inch strands made of seven Ø7 mm wires are described. In the central region, 6 similar cables (total  $A_{sp}=4849$  mm<sup>2</sup>) were located at the bottom slab of the box deck section, in correspondence to each beam. The upper and lower pre-compression cables do not appear to be overlapping, but rather leaving limited portions of the deck reinforced by the ordinary reinforcement alone.

From a flexural point of view, simple hand calculations indicate that the capacity of the deck section is adequate, without much conservatism, in the regions of maximum moments, both positive and negative. However, in the regions next to the point in which a zero-moment value is predicted (depending on the loading condition), the capacity is largely dependent on the positive effect of the compression force originated by the stays' force horizontal component, with limited ability of absorbing any moment inversion due to unexpected actions. It is evident that the deck would not have been able to resist even its own weight without the restraining action provided by the cable; for this reason, during the construction phases when the stays were not yet present or active, the presence of the temporary cables, later removed, was essential.

Shear reinforcement was provided in a rather customary fashion, with varying numbers of stirrups and different diameters. In regions close to the stay connections, it appears that Ø14 mm and Ø8 mm stirrups were provided at a spacing of 200 mm. In other parts, two Ø12 mm stirrups were provided at a spacing of 250 mm. Again, according to simple hand calculations, the capacity seems to be in excess of the expected demand.

### Transverse Link Girders

The transverse link girders that should transmit the load from deck to stays and from deck to pier struts are not described in any detail, but appear to be hollow sections with external dimensions in the range of  $4.5 \times 2.0$  m. The thickness of their concrete shell looks like being in the range of 0.5 m, with the exception of the bottom of

the stays girder, which seems thicker, in the range of 1.0 m. Since these measures have been visually deduced, they should be treated with some caution. No detail is available about reinforcement and pre-stressing, if any. As a consequence, a possible failure initiated in these transverse girders cannot be excluded, but is thus not addressed in the present work.

### Cable Stays

According to the original design (Fig. 5), each cable stay contained a total of 464 strands with nominal diameter of ½ inch, of which 352 were located first and connected to the deck to bear its dead weight. Then, the concrete section was cast and the remaining 112 strands were used to post-compress it. Finally, all ducts were stated to be injected and the cables connected to the deck. The design hypothesis was that the stays concrete would remain in compression under the application of the full dead and live load, simply supported spans included. The calculations that follow, however, do not necessarily confirm such design assumption.

Considering the geometry of the deck and some reasonable assumptions regarding material weights, the force in each cable stay due to the self-weight of the deck is estimated at around 12 000 kN, which increases up to a total of about 22 500 kN when considering the simply supported Gerber spans and adding the dead loads (DL, about 10 500 kN added). A reasonable estimate of the maximum cable force due to live loads (LL, if one considers the specifications at the time of construction; today the estimate will likely be 50% higher) is in the range of 4000 kN. The concrete ( $A_c$ ) and steel ( $A_s$ ) areas are about  $A_c = 1\,073\,776\text{ mm}^2$  (depurated of the ducts area),  $A_{s352} = 32\,700\text{ mm}^2$  (considering the 352 ½ inch tendons originally connected to the deck) and  $A_{s112} = 10\,404\text{ mm}^2$  (considering the 112 tendons used to compress the concrete). The post-tensioning stress adopted is not clearly stated and will be assumed as  $\sigma_{p,s} = 900\text{ MPa}$  after losses. In this case, assuming perfect bond, the expected stress values in concrete and steel in the subsequent phases of construction may be estimated as follows:

Phase 1	Deck connection: 12 000 kN on 352 tendons	$\sigma_{s352} = 367\text{ MPa}$
Phase 2	Post-tensioning at 900 MPa on 112 tendons	$\sigma_{s112} = 900\text{ MPa}$
		$\sigma_c = -8.7\text{ MPa}$
Phase 3	Addition of supported span and DL: 10 500 kN	$\sigma_{s352} = 367 + 75 = 442\text{ MPa}$
	(assuming a ratio between elastic moduli $E_s/E_c = 10$ )	$\sigma_{s112} = 900\text{ MPa}$
		$\sigma_c = -8.7 + 7.5 = -1.2\text{ MPa}$
Phase 4	At the extreme condition of maximum LL: 4000 kN	$\sigma_{s352} = 436 + 28 = 464\text{ MPa}$
		$\sigma_{s112} \approx 900 + \text{MPa}$
		$\sigma_c = -1.2 + 2.8 = 1.6\text{ MPa}$

The concrete stress state estimate shown above for Phase 4 seems to imply that there was a need for an increase in the steel strands tensile stress to compensate for the concrete contribution beyond decompression. However, the above calculations need to be considered with care, for several reasons: (i) the assumptions made

about the post-tensioning force and the elastic moduli ratio; (ii) time dependent effects are not considered; and (iii) the previously noted unlikely injection of the cable ducts (which would imply absence of bond between steel and concrete). Whilst a certain conservatism in the design is undoubtedly present against a stay collapse (the steel tendons alone would be able to take the entire maximum load at a stress of about 600 MPa, with a safety factor of around 2.8), potential concrete cracking is indicated by the possible tensile stress up to 1.6 MPa.

As such, even though the abundance of the steel capacity has possibly played a role in avoiding premature problems, the potential for concrete cracking and the absence of grouting may have induced relevant variations in the bridge stiffness, as well as in periods and modes of vibration. The absence of injection, in particular, may have resulted in the following effects:

- (1) In the case of bonded tendons, the concrete may be able to sustain a tensile stress of 1.6 MPa and, even in case of cracking, tension stiffening would contribute to reduce the cable elongation. In case of lack of bonding, instead, the concrete part would not absorb any tensile force and the stiffness would reduce to that of the tendons alone;

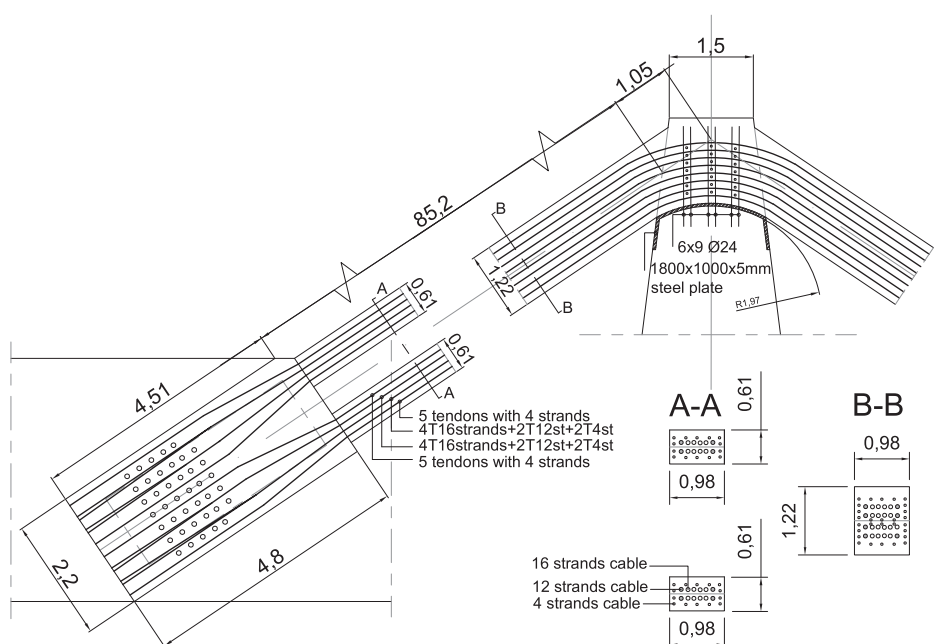


Fig. 5: Geometry and reinforcement of the cable stays (Units: m)



- (2) Similarly, in the case of bonded cables, a local fracture of some wires would possibly result in the local opening of a visible crack, without losing the compression force in the remaining part of the stay concrete. On the contrary, in the case of unbonded cables, a progressive reduction of the steel section, hence of the corresponding post-tensioning force, would not necessarily induce cracks, but rather a global elongation and loss of compression in the entire stay concrete;
- (3) The details of the strands at the top of the pier, simply curved on a saddle, not connected to cable heads, had to sustain millions of cycles with a small flexural component, rather than tiny oscillations of the tensile force;
- (4) The sensitivity to the aggressive marine environment and the consequent potential corrosion of the strands became much higher.

The combination of the presence of tensile concrete stress and absence of bond, together with the possible deterioration of the steel tendons and the consequent reduction of the compression force in the stay concrete, may have resulted in increased deformability and a consequent different distribution of shear and bending moments, leading to a decreased force in the cable and increased reactions at the pier struts and in the corresponding deck shear.

### Supported Spans

The simply-supported spans were constituted by six precast pre-stressed Gerber beams connected by an upper slab (Fig. 6). The maximum depth of each beam is 2.20 m, plus the cast in place slab (depth of 0.16 m). From the available drawings, it appears that 10 cables were used, each made up of 18  $\varnothing 7$  mm wires. Consequently, the total pre-stressing force, after losses, can be estimated in the range of 6235 kN, considering a 900 MPa average stress. In the central section this would result in a pre-stressing bending moment in the range of 6235 kNm, considering the beam depth only (i.e. without the collaborating slab). From hand calculations, this bending moment value seems to be very similar to that originated at mid span by the total self-weight and dead loads acting on each beam. This seems quite consistent with the final increased depth and strength and a maximum potential increment of the acting bending moment in the range of 30% due to live loads. For what concerns shear reinforcement,  $\varnothing 10$ ,  $\varnothing 8$  and  $\varnothing 6$  mm diameter stirrups at 200 mm spacing were provided.

### Structural Assessment, Strengthening and Monitoring from the 1990s Onwards

In the early 1990s, “during maintenance and repair activities, it was discovered that the stays of the three balanced

systems were suffering from widespread general deterioration, as well as several instances of concentrated degradation”.<sup>27,28</sup> The papers describing the situation are focused on the strengthening intervention on pier 11 (East bound, towards Genoa) and do not provide much detail about the findings on corrosion and cable injection. Whilst the strengthening intervention is of limited interest herein (though it may shed light on the state of damage), the fast pace at which decisions were taken and strengthening (on pier 11) was implemented, is an indicator of the gravity of the state of deterioration. The same worries can be inferred by the decision of transferring the entire stays capacity to new external cables, maintaining the existing post-tensioned elements only for convenience of the strengthening workflow and to favour a more progressive transfer of the forces.

A photograph taken at the top of the antenna after removing the concrete cover seems to confirm a complete absence of any injection and some corrosion. In the aforementioned publications, it is also described how the emission of high-frequency impulses at one end of a cable and their recording at the same place upon reflection can be used to acquire data about defects in the cable, as well as some measure of the tensile force present in the strand. However, the general impression is that once it was decided to essentially replace the stays, there was no interest in

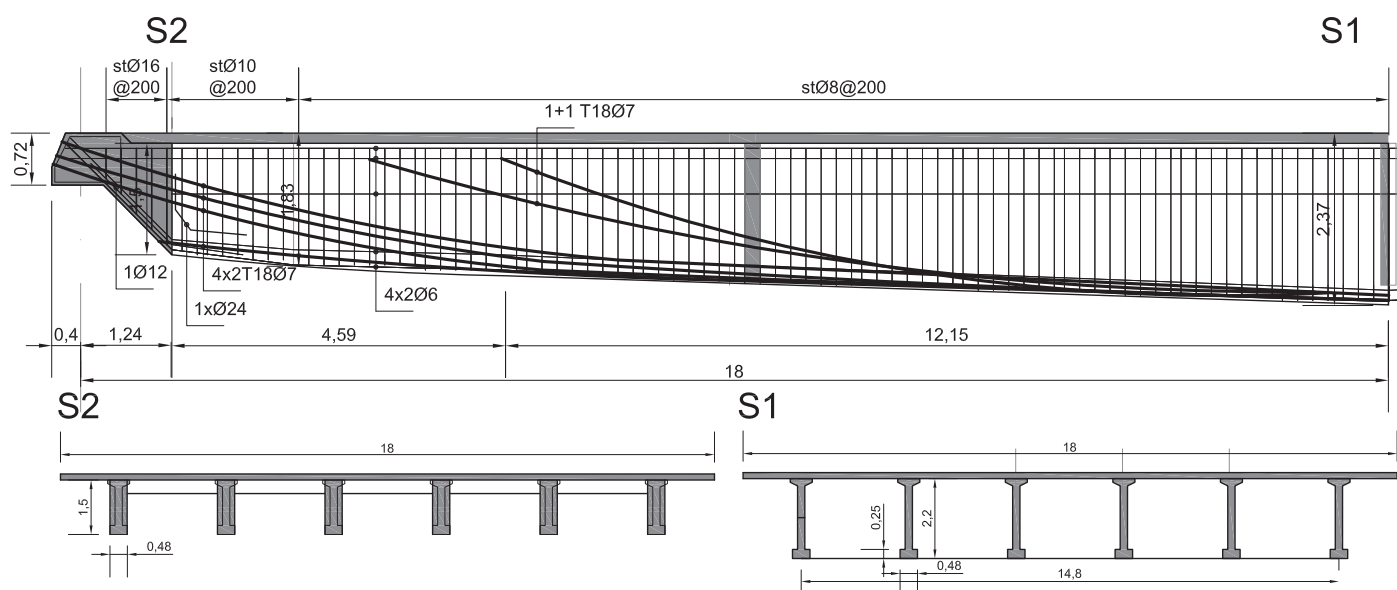


Fig. 6: Geometry and reinforcement of the supported span (Units: m)

gaining a deeper and detailed understanding of the actual situation in which the bridge found itself in (for instance, and as a minimum, it is very likely that a dynamic identification of the system response would have indicated the presence, or absence, of bonding between cable and concrete, but this does not seem to have been pursued).

For pier 10 it was concluded that “the criticalness was mainly concentrated in the sections stretching to the cross-beam at the top of the tower, and hence the interventions were limited to these areas”. For pier 9, now collapsed, it was concluded that “the stays are in better condition due to the more limited corrosion present in both primary and secondary cables. Hence no intervention of any type is scheduled”. As a safety measure, “control over time of the state of conservation of the pre-stressing cable is assured through the installation of a system of continuous reflectometer control” and the conclusion was that “from an estimate of the intervention time limit, and considering the empirical laws which govern the speed of degradation, the limit condition is estimated to be around 2030”. Leaving aside the somewhat intriguing nature of this conclusion (particularly for what concerns the definition of “the limit condition”), it appears clear that:

- Pier 9 was not the object of any strengthening measure, not even locally;
- The attention was focused on the stays, not on the deck, transverse links, supported spans or pier elements.

However, the report of the *Commission of the Ministry of Infrastructures and Transportation*<sup>26</sup> describes an intense structural monitoring activity in the years that followed the above retrofitting, with inspections on all main elements of the bridge, along with further repair and strengthening interventions. Whilst the discussion in such report about alleged delays in intervening is not of interest here, the following aspects may instead carry some relevance to the current work, with reference to the implications on the structural modelling:

- (a) The absence of any injection mortar is repeatedly evident both in the stays and the deck cables;
- (b) Presence of oxidation and

corrosion is also reported in most of the examined reinforcement, with estimated extension between 10 and 30% (2015);

- (c) In some cases, an apparent loss of post-tensioning is reported, with some strands free to move (2011–2015);
- (d) In two cables, made visible in a precast beam, “no fewer than four wires were fractured” and “all wires were movable by hand” having thus lost any tensioning (2011);
- (e) In a series of dynamic identification tests, seemingly inconsistent responses of different stays have been reported and ascribed to differences in progression of corrosion and loss of post-tensioning. The identification of four natural vibration periods in the range of 0.70–0.82 s is reported, but no correlation with numerical models and related assumptions is described (2017).

The above observations are clearly indicative of a general state of deterioration of the entire structure, and whilst they do not allow one to precisely define deterioration on an element by element basis, they did assist in the identification of potential weak links and critical scenarios, evaluated in the subsequent sections.

### Estimation of Member Demands and Assessment of Capacity

The “balanced system” under consideration is nominally symmetrical around both the longitudinal and transverse axis, hence, from a numerical analysis point of view, it is irrelevant to discuss on which side of the system the collapse has been originated. However, the position of the debris (slightly located on the north side of the viaduct on the western side) seems to indicate that the south-west side stay should have been released first. Furthermore, the only heavy vehicle (a red truck transporting a steel coil) travelling across the bridge at the time of the event was driving on the south lane, towards Genoa, and the driver reported that he perceived an initial collapse behind him. One can thus assume, while keeping the aforementioned considerations on double symmetry, that the first stay to release its restraining capacity to the deck was the south-west one.

Whilst it can be considered unquestionable that a stay (and, as discussed above, most likely the S-W one) must have released its retaining capacity at a certain point of the collapse sequence, the question remains on what might have been the triggering cause and the ensuing progressive sequence of events. A few alternative hypotheses have been considered in this study (based mainly, though not exclusively, on the observations described in the third section above):

- (a) A first possibility is the simple progressive deterioration of the stay strands, with a progressive fast elongation or a fatigue collapse that induced a migration of the tensile force in the parallel stay on the opposite side of the viaduct, with a consequent in-plane rotation of the deck and a concurrent torsional effect. In this case, there is no solid estimate of the exact time of the event, apart from the small load increment due to the passage of the heavy vehicle;
- (b) Considering that the shear strength of the deck in the intermediate region was largely counting on the compression induced by the stays, another possible sequence of events is given by the combination of elongation of stay cables, shear/torsion collapse in the deck and consequent complete failure in the stay. Note that the mentioned unbonding of the cables may have favoured this failure sequence, as pointed out earlier;
- (c) A third hypothesis is a possible local failure in some part of the deck, which may have led to the cable collapse. This may have been induced, for example, by a loss of post-tensioning in the terminal cantilever element, with a consequent shear collapse and loss of support for the simply supported span. Other local failures could be those at the stay-deck or stay-antenna interfaces;
- (d) The collapse could also have been originated by shear failure of the simply supported span, in the region next to the Gerber saddle, triggered by a local impulsive load such as the tumble of a steel coil from a heavy vehicle’s trailer (though no evidence of this event has so far been publicly reported). In such a case, the resulting

sudden release of the applied force on the main deck and corresponding stay, together with a migration of the compression force to the adjacent beams and the consequent torsional effects, could have caused failure in the main deck and in the stays.

All the hypothesised mechanisms above have been examined and their relative likelihood of occurrence has been assessed, developing first a BIM model to ensure a common interpretation of geometry and reinforcement in the development of the different structural models that are described below.

### Estimation of Member Demands

#### Elastic Static Analysis

The structural analysis software SAP2000<sup>29</sup> was used to develop a linear-elastic model that would properly reproduce the sequence of construction and applied loads. Five stages were considered, as described in what follows and illustrated in Fig. 7:

- (1) The pier, the antenna and the central span of the deck are modelled by *frame* and *shell* elements, which are under their self-weight only, as applied load;
- (2) The complete deck is added together with the four stays with an area corresponding to the 352

½ inch tendons. The stays are modelled with *cable* elements and provided with an initial tension strain corresponding to about 140 mm total shortening, so as to obtain an approximately zero vertical displacement once the supported spans and the dead load are added. This is the same procedure described by Morandi during the bridge's actual construction. At this stage, the resulting axial force in each stay is about 12 300 kN and the total vertical reaction at the pier base is about 170 MN. The vertical deck displacements vary between 96 mm (upwards, at the cantilever tip) and 120 mm (downwards, approximately at mid span);

- (3) The post-tensioned cables and their concrete casing are added to the stays, in parallel to those considered in the previous step. The total vertical reaction is about 177.6 MN, consistent with the total weight assessed by the BIM model;
- (4) The supported spans and the dead loads (2.4 kN/m<sup>2</sup> and 18 kN/m for the three longitudinal lines of New Jersey barriers) are added. The axial force in each stay increases to a total of 22 600 kN (13 600 kN taken by the original 352 tendons and 9000 kN by the post-compressed concrete element). The total vertical reaction is about 212.4 MN.

At this stage, which is the final one excluding live loads, the compression force in the deck, due to the stays action only, varies between 21 000 and 28 500 kN. The addition of the live loads does not induce major changes, with maximum action increments in the range of 5–20%, depending on the element considered. The element where the variation is more relevant is the post-compressed concrete part of the stay, with an increase in the stress from 9000–12 000 kN. The corresponding deck displacement is between 5 and 6 mm, making it essentially irrelevant. The final tensile stress in the 352 original tendons varies between 650 and 750 MPa;

- (5) The S-W stay is removed (without considering any applied live load), to check if the structure would have been able to find equilibrium in this situation (it is noted that the removal of the S-W stay implies also the immediately subsequent loss of its S-E counterpart, given that, as discussed before, the cable is a continuous element passing over a saddle at the top of the antenna, without any local restraint). The resulting bending moment diagrams showed, as expected, a sign reversal in the external deck ribs on the side of the missing stays, incompatible with the beams capacity and a high bending in the horizontal plane, acting mostly on the stays diaphragm. The axial force in the remaining stays increases to about 39 000 kN, still compatible with the cable capacity, but the vertical displacement exceeds 400 mm on one side and 1 m on the other, which is incompatible with the presence of the supported beam. At the base of the balanced system, the overturning moment in the transversal direction is about 918 MNm, with an equivalent eccentricity of 4.5 m. Consistently with the deck vertical displacement, a temporary situation, in which one side of the supported span collapses, has been considered. In such case, a longitudinal base overturning moment of 307 MNm is observed, with an equivalent eccentricity of 1.55 m. Both eccentricities do not appear to induce relevant tensile forces in any element.

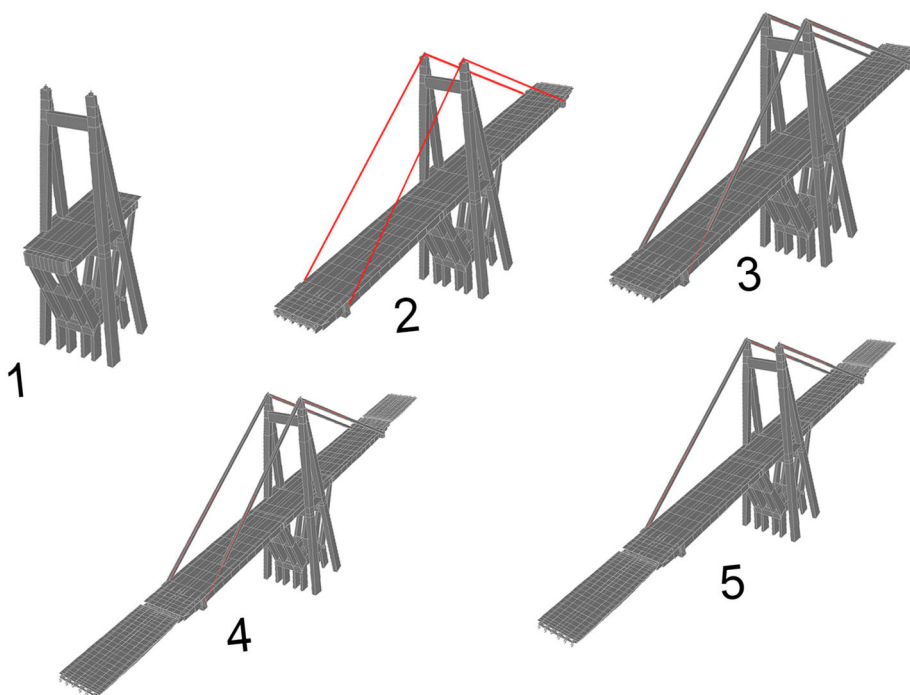


Fig. 7: Illustration of the four construction stages adopted for the modelling (aligned with the bridge's actual construction sequence), plus the case where the S-W stay is removed

Whilst a comparison of demand and capacity at the main critical sections will be addressed later on, it is anticipated that no significant problem seems to occur in any as-designed element of the bridge, considering also the described sequence of construction and loading and consequent internal restraints. Time dependent effects have not been considered; however, even if they might have induced increased deck displacements in the stays connection regions, migration of shear forces towards the pier struts or irregularities in the road level, it is unlikely that these aspects have played an important role in the observed collapse of the bridge, as further discussed in subsequent sections of this paper.

### Time-history Dynamic Analysis

Further investigation of the elastic behaviour, considering also dynamic analysis, was carried out using a model developed in OpenSees.<sup>30</sup> As in the case of the SAP2000 model, this was initially modelled using elastic elements with the aim of analysing the sectional demands along the bridge deck at the various construction stages and for potential loading situations. The basic assumptions regarding the geometry, material properties and construction sequence were identical to that of the SAP2000 model. Each of the four stages of construction outlined above was followed and similar results between the two models were observed, which was reassuring. For example, at stage 2, when the 352 cables are added and tensioned to bring the deck to a horizontal position under its self-weight, an initial axial deformation of 0.145 m was required. In fact, it was observed that had these stays not been added and the deck left to work as a simply supported cantilever, an end displacement of over 1.2 m would have resulted, highlighting the need of constructing the deck segmentally with temporary restraints as described. Once the 352 cables were added and tensioned, their axial force was reported as 12 575 kN, similar to what had been obtained also with the SAP2000 model. Following this, the rest of the stay elements were included, the Gerber beams added and the live loads considered. The final axial force observed in each cable was 22 359 kN, which again is similar to the SAP2000 modelling case, in addition to a maximum shear demand of 12 574 kN and sagging and hogging bending

moment demands of 88 590 and -110 696 kNm, respectively.

Subsequently, starting with the OpenSees model described above with each of the elements modelled as linear-elastic but with the possibility of defining inelastic elements if/where elastic capacity would have been reached, the increment in forces for dynamic loading due to the applications of a series of ground motions was analysed. The mass of the bridge elements was modelled as continuous mass and the static loading scenarios included as constant gravity loads. The seismic action was that stipulated by the 2008 Italian design code,<sup>31</sup> with reference return periods of 120, 201, 1808 and 2475 years being adopted for the operational, damage limitation, life safety and collapse prevention limit states, respectively. These assume a bridge structure with a 100-year nominal life and the maximum importance class (IV) that amplifies nominal life by 2.0 to a reference period to 200 years, since the bridge can be classed as being of public function and strategic importance. Soil type C, corresponding to a soil shear wave velocity between 180–360 m/s, was also considered. For the collapse prevention limit state, this resulted in a peak ground acceleration of 0.184 g.

Whilst all intensity levels were analysed using a set of ten spectrum-compatible accelerograms at each intensity, only the collapse prevention limit state results are discussed herein since it is the maximum potential force increase that is of principal interest here. The fluctuations in cable axial force, deck shear and moment were recorded and are discussed with respect to the section capacities computed in the following sections.

### Verification of Critical Sections

#### Flexure Capacity of Main Deck and Supported Spans

Following the calculation of the bending moment and shear force demands along the deck and simply-supported span for the different construction stages, moment and shear capacity analyses at the most relevant locations were carried out. Such critical sections were identified in correspondence to peak demands or discontinuity points (pier support or cable-stay connections) and the sectional analysis program Response-2000,<sup>32</sup> which calculates the full load-deformation

response of reinforced cross-sections subjected to shear, moment, and axial load, was employed. Considering the double symmetry of the deck's cross-section and taking into account the restrictions of the software, a simplified strategy was adopted, analysing one single I-beam portion of the complete section, formed by a five-sector box. The total bending moment capacity of the deck cross-section was therefore considered to be six times the capacity of the analysed single I-beam.

Three critical locations were considered for the verification of the bending moment capacity of the main deck cross-section, namely: (1) at the support provided by the main pier; (2) at the connection with the cable-stay; and 3) approximately at mid-span between the pier-deck connection and cable-stay-deck connection (sections 1 and 2). Using moment-curvature analysis, both positive and negative bending moment capacities were estimated for the deck cross-section at the aforementioned locations, to consider eventual moment demand reversal caused by the different described collapse mechanism possibilities. The moment-curvature responses of the three identified critical sections are presented in Fig. 8.

The comparison between the bending moment demand and capacity in the main deck is illustrated in Fig. 9, from which it can be seen how the capacity foreseen by the original design is well enough to cover the demand stemming from all the loading stages, as well as the increase originated by the consideration of the seismic loading. Even in the case of a stay removal on one side of the balanced system, it is quite clear that no flexural problem would arise. In addition to the verification of the main deck, the corresponding bending moment profile was also estimated along the simply-supported

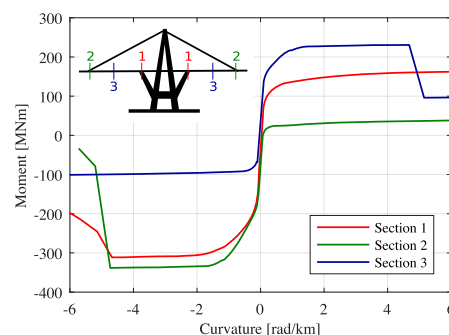


Fig. 8: Moment-curvature response of the considered deck cross-sections

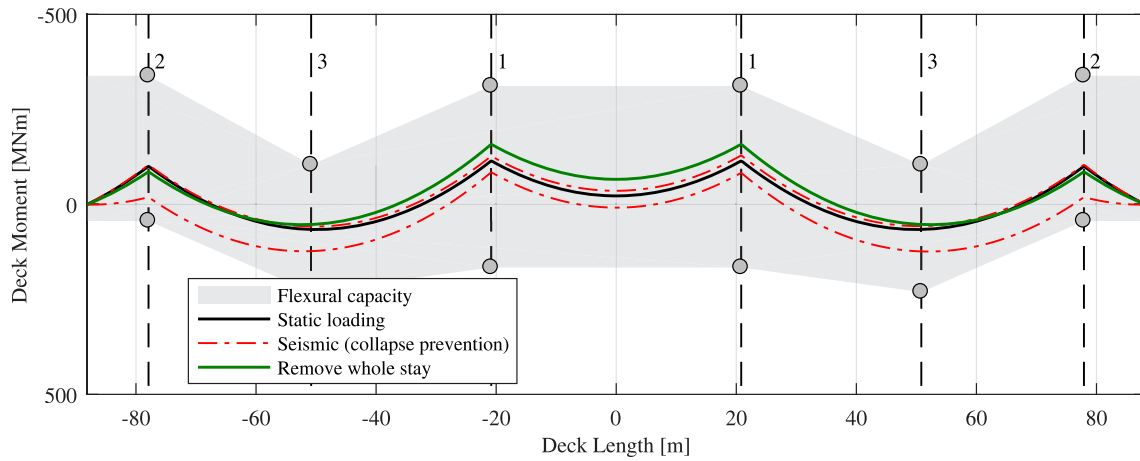


Fig. 9: Comparison of the bending moment demand along the deck with respect to the section capacities computed from moment curvature analysis

Gerber beam. Fig. 10 shows this demand, together with the capacity, and it can again be seen that there is a good degree of reserve capacity in each loading scenario investigated.

#### Shear Capacity of Main Deck and Supported Spans

The shear capacity estimates are based on a simplified version of the Modified Compression Field Theory (MCFT), formulated by Vecchio and Collins.<sup>33</sup> The MCFT represents a generalised approach for modelling the behaviour of reinforced concrete elements subjected to multi-axial loading conditions. It consists of a smeared, rotating crack model that treats stresses and strains in a localised average sense, and allows their reorientation as a result of changing load and/or material response. Similar to the case of the flexural capacity, the shear resistance of the main deck was computed at various points and is compared with the

demand for the various load cases in Fig. 11. As in the case of flexure, the shear capacity of the main deck is well above the maximum anticipated demands from both the static loading and also the seismic loading, indicating that it had sufficient reserve capacity. Furthermore, for the case of removal of the stay on the left-hand side, it can be seen that the shear demand in the deck over the left pier does not exceed the capacity, indicating that should a stay be removed from the system, no problems would be expected as a result of the increased shear demand.

With respect to the simply-supported Gerber beam, the corresponding shear force capacity profile was also estimated for different cross sections, located at 2, 9 and 18 m distance from the support ledge, connecting the main deck and the simply-supported Gerber beam. The shear capacity is depicted, together with the demand, in Fig. 12. Again, it can

be seen that there is a significant reserve of capacity in each loading scenario investigated.

For what concerns the possible accidental point load, mentioned at the beginning of this Section, a preliminary assessment, described in the paragraph below, has been carried out, leaving a more refined analysis to future detailed studies, given that not only is an impact analysis of such a complex system and the evidence very complex and time-consuming, but also because, as discussed later, even a complete collapse of the supported span would hardly result in the global collapse of the system

Assuming a weight  $W$  tumbling on the deck from a height  $h$ , the equivalent force can be estimated equating the potential energy at the beginning of the event and at maximum displacement ( $d$ ) of the impacted section, obtaining, assuming perfectly elastic

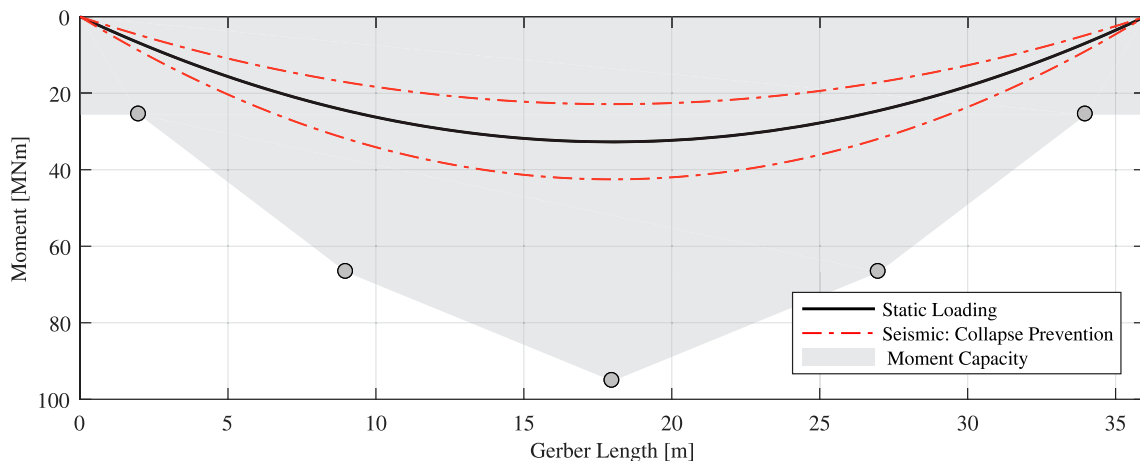


Fig. 10: Comparison of the flexural capacity of the simply-supported deck computed from moment-curvature analysis with the static loading and seismic demands

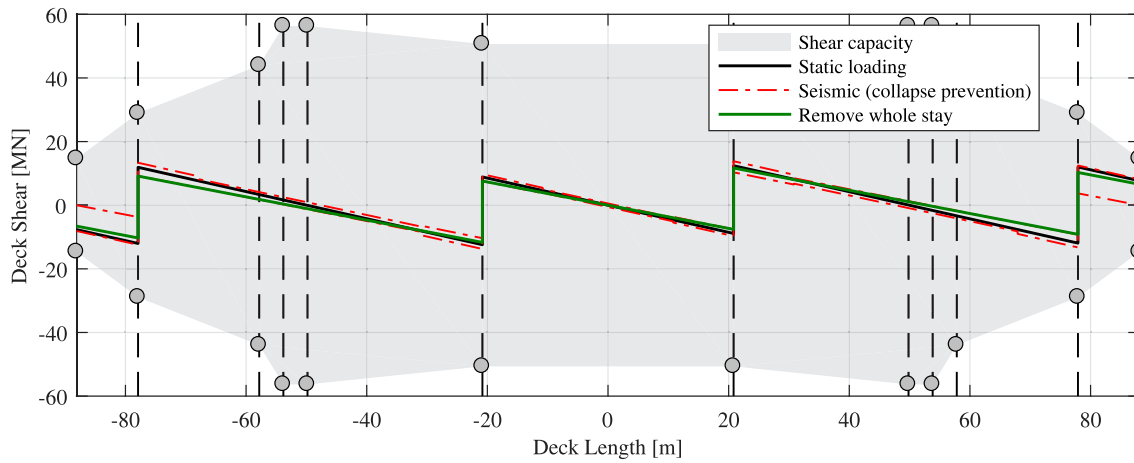


Fig. 11: Comparison of the shear demand along the deck with respect to the section capacities computed using modified compression field theory

response,  $P_e = W \cdot h/d$ . In case of an elastic response and of a falling height of the order of 1 m, this equivalent force can be in the order of ten times the tumbling weight and should be further amplified to consider the dynamic response of the structure, as a function of the ratio of the duration of the impulse and the structure proper period; as well known, the maximum amplification factor is equal to 2. It is noted, however, that considering the shear and flexural capacities depicted above (Figs. 10 and 12), it results evident that a nonlinear response is to be expected, implying damage, larger displacements and added energy dissipation, implying that a correct estimate of the impulsive load cannot be obtained by the simple use of the equation described above, valid only in the elastic domain.

A collapse induced by an impulsive load on the main deck has to be excluded, considering its large shear strength (in the range of 50 MN, Fig. 11) and considerable displacement

capacity (in the range of hundreds of mm). The only possible events are a complete punching of the upper and lower slabs, of little interest here, and a collapse of the cantilever part of the deck, in proximity of the Gerber saddle, which will produce similar effects to the saddle collapse itself, discussed later. It is noted, however, that if such impulsive action would damage the transverse link, it could have an impact in the stay-deck connection, something that would instead be of relevance, as shown later in this paper.

A shear verification of the support ledge, connecting the main deck and the simply-supported Gerber beam, was also carried out. The shear strength of the ledge was estimated using two approaches: i) strut-and-tie method, to ensure that no crushing of the diagonal struts or failure of the ties (in this case represented by the cables) would occur; and ii) interface shear transfer equations, to ensure that no interface failure would occur. These calculations resulted in a

shear capacity of the ledge estimated as 3805 kN, which corresponds to a safety factor of 4.6, when considering the shear demand due permanent loads (820 kN), but may again imply a local failure when considering the aforementioned hypothetical accidental point load acting, in addition to the permanent loads, at the most unfavourable location.

#### Torsion Capacity of Main Deck

Considering the large in-plane bending and torsion resulting from a potential stay release, the strength of the deck was also evaluated considering the simultaneous presence of torsional, shear and flexural actions. To this end, the “Variable-Angle Truss Model” proposed by Rabbat and Collins<sup>34</sup> implemented in the CSA A23.3-14<sup>35</sup> was employed. In this model, the cross section is idealised using four parallel longitudinal chords, made of longitudinal pre-stressing steel, reinforcing bars and concrete. The chords are connected by four “walls”, consisting of diagonally cracked concrete and transverse

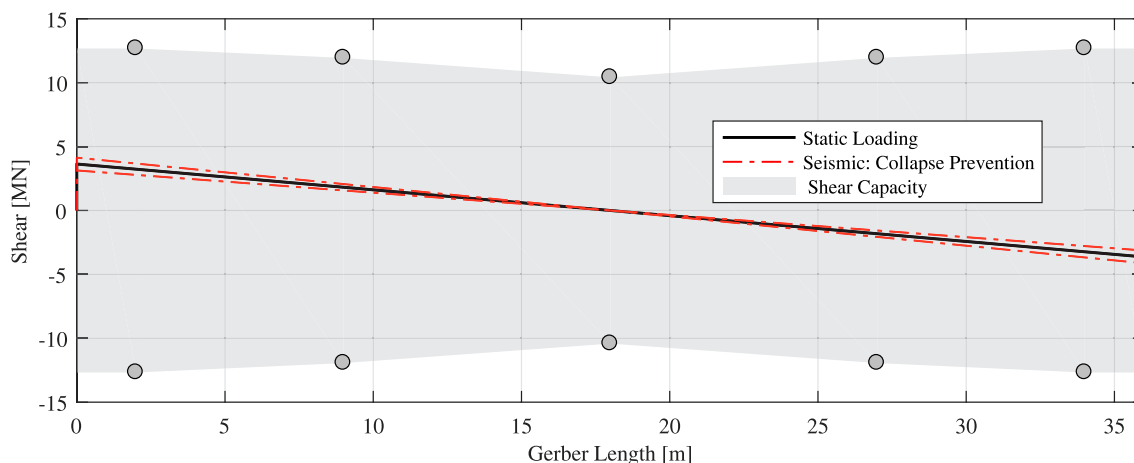


Fig. 12: Comparison of the shear capacity of the simply-supported deck computed using MCFT with the static loading and seismic demands

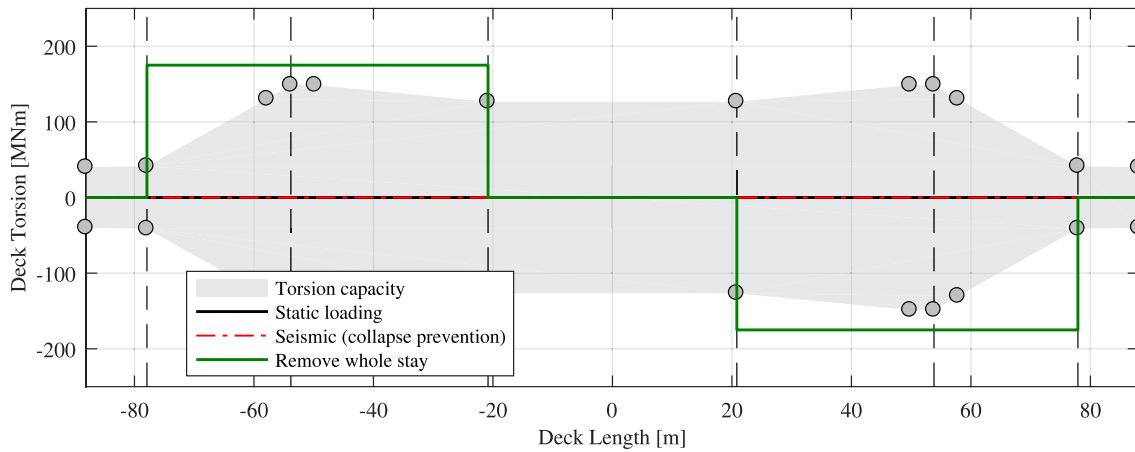


Fig. 13: Torsional capacity, computed both under normal and post-stay removal loading conditions, at various points of the main deck

reinforcement. Moment and axial forces acting on the cross section are resisted by axial stresses that arise in the chords, while shears and torsions acting on the cross section are resisted by shear flows that develop in the walls. In performing the calculations, a simplifying assumption was made that is the shear flow generated by an applied torque was assumed to distribute only along the perimeter of the cross section, thus weighting only on the flanges and on the two most outer webs.

As before, the torsional capacity was computed for a number of sections along the main deck, as shown in Fig. 13. For what concerns the torsional demand, Section 4.1.1 reported that upon the removal of one of the stays, the forces increased from a balanced 22 600 kN in each stay to about 39 000 kN in a single stay. Considering that the upward force in the remaining stay is now unbalanced, this would be anticipated to translate as a torsional force in the main deck. Taking the vertical component of this 39 000 kN axial force as half, given the stays are inclined at approximately 30°, and multiplying by the lever arm of half the deck width, taken as 18 m, the estimated torsion induced along the main deck is about 175.5 MNm, which was reported by the numerical model and shown in Fig. 13. In addition, the eccentricity of the axial force in the plane of the deck will produce an in plane bending moment, which can be estimated in the range of 250 MNm, with simple equilibrium consideration similar to those applied for the torque. The torsional demand alone, following the stay removal, is far in excess of the torsional capacity computed under normal loading conditions (Fig. 13), and will be worsened by the additional tensile and

compression forces resulting from the in-plane bending moment. Therefore, a torsional failure of the deck following the rupture of the stays on one side represents a plausible sequence of events.

#### Seismic Capacity of Pier and Antenna

In addition to the deck elements, the forces acting in the antenna were also checked to ensure that it too possessed sufficient reserve capacity for the situations examined here. For the static loading with the self-weight and live loads, the vertical force acting through each antenna leg is found to be 27 100 kN, which when considering the cross section to be 4.5 × 0.9 m, gives an axial load ratio of  $v \approx 0.18$ , computed as the axial load normalised by the product of the gross cross-sectional area and concrete compressive strength, taken as 37 MPa. For the case when the whole stay is removed on the south side, the forces acting through on the antenna legs on the same side reduce, with the opposite legs being compressed further. The maximum compressive load through the antenna legs on the north side increases to 32 300 kN, which gives  $v = 0.22$  and the maximum load on the side with the stay removed reduces to 17 400 kN, giving  $v = 0.12$ , which confirms that the legs of the antenna would be expected to remain in compression despite losing a stay.

In the case of the seismic loading, the axial load ratio in each antenna leg for the collapse prevention limit state intensity increased from the  $v = 0.18$  reported above to a value of  $v = 0.21$ . For the case of the pier legs, under normal loading conditions the axial load ratio is computed as  $v = 0.05$  in each leg, but when examined under seismic loading increases to a

maximum value of  $v = 0.11$ . These values suggest that for both normal and seismic loading conditions, neither the pier nor the antenna exhibit any cases of relatively large loading nor would they have presented any alarming results had a seismic verification been examined.

#### Summary and Preliminary Conclusions

An examination of the outcomes of the analyses and verifications described above already allows one to derive a number of preliminary considerations. In general, the “balanced system”, as conceived and designed, appears to have had significant capacity reserves, as demonstrated by the large force/moment capacity-demand ratios in flexure, shear and torsion mechanisms.

Indeed, and more specifically, it seems that the complete loss of a stay could have resulted in the type of complete collapse that was observed, given that:

- The flexural and shear capacities of the deck are in the range of two or more times the demand under normal loading conditions and may even sustain the impact of a stay removal;
- However, a stay removal will induce a bending moment in the plane of the deck and a torque that will be above the capacity (Fig. 13);
- The live loads are only a small fraction of the permanent loads and cannot change significantly the stress and strain demand.

However, it cannot be excluded that an impact on the deck induces local damage and possibly attains the capacity of one or more of the beams of the simply supported span, though

not necessarily implying a global collapse. Local failures may have been favoured by the combination of significant deterioration of some tendons (i.e. a significant reduction of their cross-section), combined with exceptional point loads.

These considerations, and others of the same nature, guided the progressive collapse analyses presented and discussed in the next section.

## Assessment and Explicit Modelling of Possible Collapse Mechanisms

The explicit representation of complete structural collapse, and corresponding formation of debris, is still an open challenge in numerical modelling. However, recent applications<sup>36–39</sup> have shown that the Applied Element Method (AEM) does appear to be able to capture adequately the progressive failure of both masonry, steel and RC structures. Originally developed by Meguro and Tagel-Din<sup>40–42</sup> to simulate controlled structural demolition and the impact of blast events, it is based on the mechanical interaction between rigid bodies connected to each other by zero-thickness interface spring layers, in which the material properties of the system are lumped. A discontinuum-based formulation therefore, that renders this approach naturally suitable for representing contact, impact and collision phenomena. In this work, the AEM-based software tool Extreme Loading for Structures<sup>43</sup> has thus been employed with a view to numerically investigate potential failure mechanisms and triggering factors that might have contributed to the observed collapse of the Morandi bridge. To this end, the influence of several parameters, including corrosion-induced deterioration of reinforcement in different locations of the bridge, have been assessed numerically through a sensitivity study.

The AEM model was assembled considering analogous assumptions to those adopted for the elastic models developed in SAP2000 and OpenSees (including the fact that only one of the three balanced systems that constitutes the bridge, the one that collapsed, was modelled). As for the previous models, therefore, each structural component was

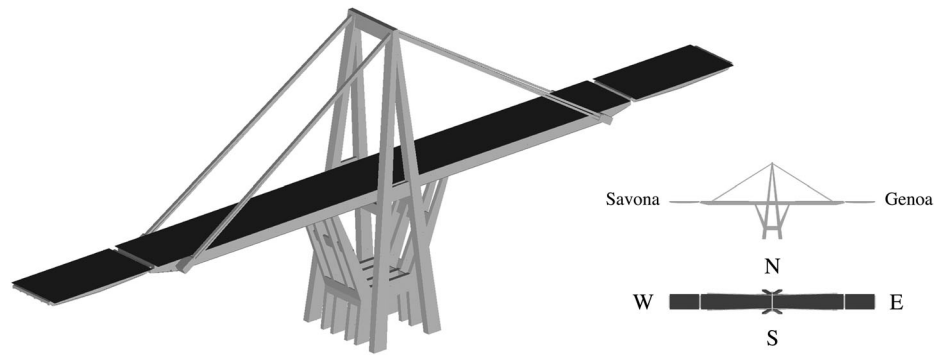


Fig. 14: Screenshot of the AEM model (320 000 degrees-of-freedom)

explicitly reproduced, as depicted in Fig. 14, including both active and passive reinforcement. The stays were modelled as an assembly of two different elements working in parallel; beam elements to represent the post-compressed concrete components, and nonlinear links to represent the pre-tensioned tendons (making sure that zero vertical displacements were obtained after the addition of the supported spans and the dead load). The complete model featured 320 000 degrees-of-freedom.

Before the undertaking of the collapse analyses, a consistency check of the AEM model was carried out by comparing the internal forces and deformations produced by the latter during the application of the static loads against their SAP2000 and OpenSees counterparts. For instance, the initial tension strain to obtain zero vertical displacement after both the application of dead load and the construction of the supported spans predicted by ELS was 148 mm (SAP2000: 140 mm, OpenSees: 145 mm), the recorded vertical reaction at the pier base was 165 MN (SAP2000: 170 MN, OpenSees: 167.7 MN), the axial force in the 352 tendons and the post-compressed concrete element was 20 800 kN (SAP2000: 22 600 kN, OpenSees: 22 359 kN). The relatively minor differences reported above were expected, given that, in addition to the conspicuously diverse underlying numerical formulation, in the ELS model the mechanical interaction between RC beams and pre-stressed reinforcement is explicitly accounted for (whilst it had been neglected in the other two models).

In what follows, a number of modelling scenarios are presented and discussed with a view to explore what possible causes could be behind the observed collapse of the bridge, noting that,

with a view to simplify the analyses, no live loads have been considered at this stage.

### Scenario 1—Progressive Deterioration of the Reinforcement in the Stays

Progressively reducing the cross-section area, as potentially induced by corrosion, of the 112 tendons providing the post-compression on the S-W concrete stay implies an equally progressive decrease of the stay's stiffness and hence progressive elongation. As discussed previously, the latter could induce a migration of shear and a torsional action in the deck that could potentially lead to the failure of the S-W stay and the consequent collapse of the bridge. However, this is something that was not observed numerically. Indeed, reducing the cross-section area of the post-compression tendons of the S-W stay all the way up to unrealistically low values, thus inducing significant changes on the axial stress of the 352 pre-tensioned cables, did not lead to a collapse of the bridge. For instance, considering a 50% tendons cross-section area reduction leads to only a  $-19$  mm additional vertical displacement at the connection between the S-W stay and the deck (and naturally even smaller vertical displacements on the N-W, S-E and N-E stays-deck connections). Considering instead a reduction of 70% (see Fig. 15) leads to a maximum displacement of  $-45$  mm on the S-W side (and  $-17$  mm N-W,  $-10$  mm S-E,  $+6$  mm N-E), which is a condition still far from inducing collapse.

Given that the reduction of cross-section area of the 112 post-compression tendons of the S-W stay alone did not lead to collapse, a number of additional cases have been



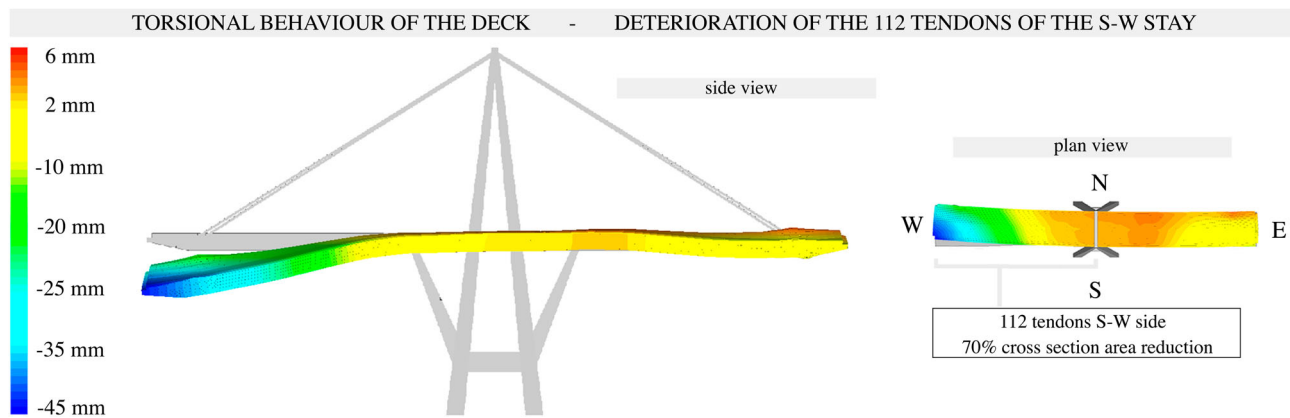


Fig. 15: Deformation induced by a 70% reduction of the cross-section area of the 112 post-compression tendons in the S-W stay

modelled assuming cross-section area reduction also for the 352 pre-tensioned cables, both in the S-W stay alone, as before, as well as in the other three stays. Even if significant vertical displacements (up to  $-800$  mm) were obtained (which would have induced noticeable progressive structural damage), in most of the cases the bridge seems to be able to cope with them, thanks to its good capacity of accommodating relative displacements and to find different equilibrium configurations through the exploitation of the large over-strength present in many elements and sections, discussed in the previous section of this paper.

As an example, considering a cross-section area reduction of 50% of both the S-W and S-E steel cables, in addition to a deterioration of 70% of the cross-section of the S-W 112 post-compression tendons, leads to a S-W vertical displacement of  $-480$  mm, whilst on the S-E, N-W and N-E,  $-240$ ,  $-250$  and  $-140$  mm were respectively predicted. Although this case was specifically selected for maximising the deck torsional response and a considerable relative vertical displacement between the S-W and the N-W side of the bridge was observed, no collapse occurred. Indeed, in order to be able to obtain an explicit collapse of the structure, an area reduction in the range of 60–70% of both the 112 post-compression tendons (S-W stay) and the 352 pre-tensioned cables (S-W and S-E stays) would need to be introduced. It is thus concluded that whilst a progressive reduction of tendons cross-section area and related post-tensioning force might have been a con-cause of the observed collapse, it could not by itself alone be the cause of the collapse of the bridge, since conspicuous signs of significant

structural distress would have had to appear well in advance.

### Scenario 2—Collapse Induced by an Impulsive Load Acting on Critical Sections

This modelling scenario explores the possibility of a collapse induced by the previously introduced hypothetical case of an impulsive load acting on critical sections, possibly weakened by some loss of post-tensioning. The aforementioned local impulsive load was thus considered acting in the vicinity of the support ledge, with an ultimate capacity of 3400 kN being obtained, when local shear failure of the occurs, albeit not leading to the collapse of the entire supported span, as illustrated in Fig. 16.

Finally, and although the simply-supported Gerber span appears to possess sufficient strength to withstand the considered hypothetical accidental impulsive load, the effect of its potential failure on the global dynamic response of the bridge was nonetheless investigated, through the sudden removal (after the application of the static loads) of one, and then two of its six constitutive Gerber beams. In the first case, no explicit collapse of the supported span was obtained. On the contrary, the simultaneous removal of two of the Gerber beams did lead to a collapse of the supported span, which induced on the main bridge system a flexural deformation producing vertical displacements at the connection between the S-W stay and the deck of  $+160$  and  $+170$  mm towards N-W and S-W respectively, whilst on the N-E and S-E sides  $-135$  and  $-145$  mm. As also gathered from Fig. 17, however, such scenario does not lead to the collapse of the bridge.

It is therefore concluded that no reasonable level of impulsive loading could cause the collapse of the bridge, unless in combination with other problems, for example, a concurrent loss in the stay capacity.

### Scenario 3—Failure of the Deck-stay or Antenna-stay Connections

As depicted in Fig. 18, two scenarios are herein considered; either a failure at the interface between the S-W stay and the antenna (possibly related to fatigue in the tendons), or the sudden loss of connection between the same S-W stay and the main deck (as previously discussed, the limited knowledge about the transverse link details cannot exclude this possibility). The collapse sequence (as induced by the antenna-to-stay interface failure) is depicted in Fig. 19; (i) a torsional collapse of the deck in a section next to the west side of the pier strut and the subsequent falling to the ground of the west supported span, (ii) the consequent release of the S-W stay and flat collapse to the ground of the west deck and supported span, (iii) the collapse of the south antenna, followed by the north one, (iv) the collapse of the central span when hit by the falling antenna debris. A very similar collapse sequence was obtained for the case of deck-to-stay interface failure.

The progressive collapse sequence described above seems to be remarkably consistent with the actual evidence, as may be gathered also from Fig. 20, where observed and predicted debris are compared. Such a good agreement seems to lend further weight to the possibility that the collapse of the bridge was indeed triggered by a failure of the deck/antenna interfaces of the S-W stay.

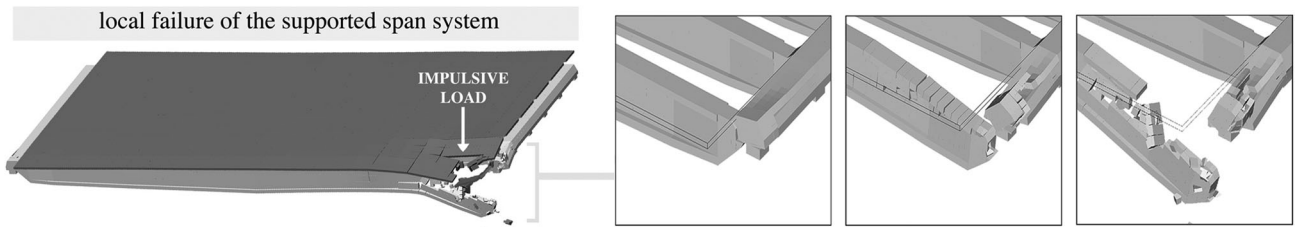


Fig. 16: Potential local shear failure in the supported span caused by an accidental impulsive loading

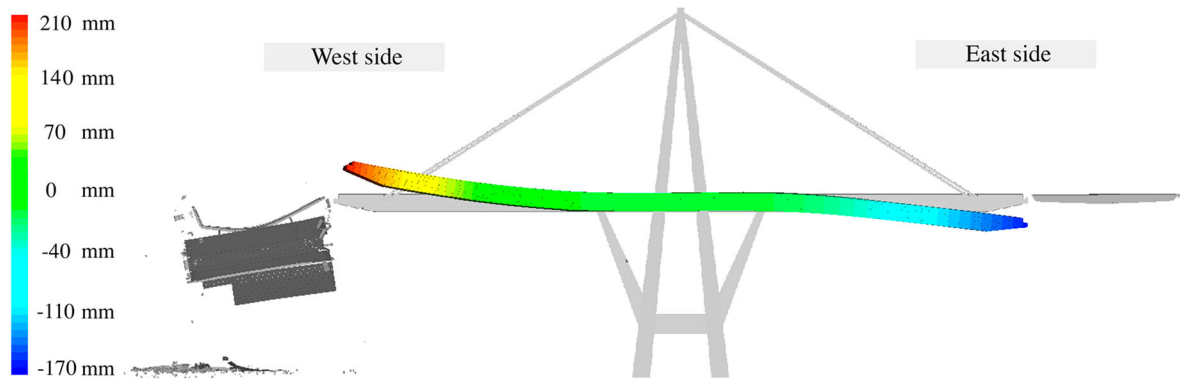


Fig. 17: Bridge response when one of the simply-supported Gerber spans is taken to collapse

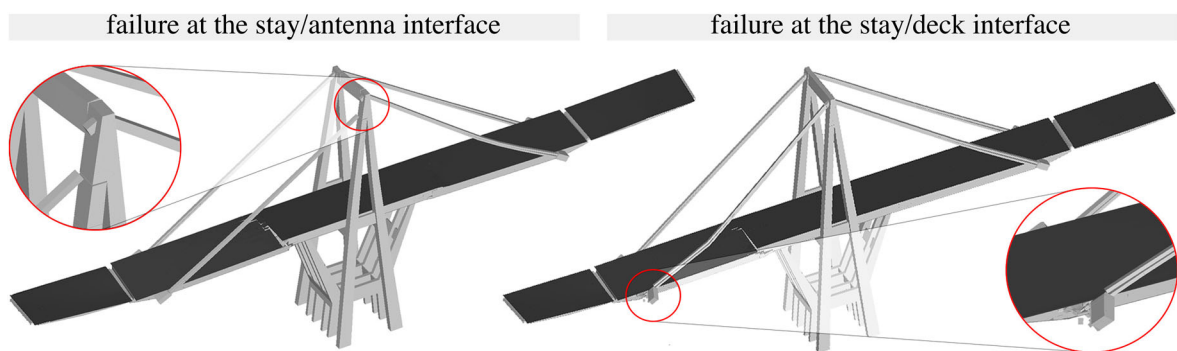


Fig. 18: Failure of the S-W stay at the interface with antenna (left) and deck (right)

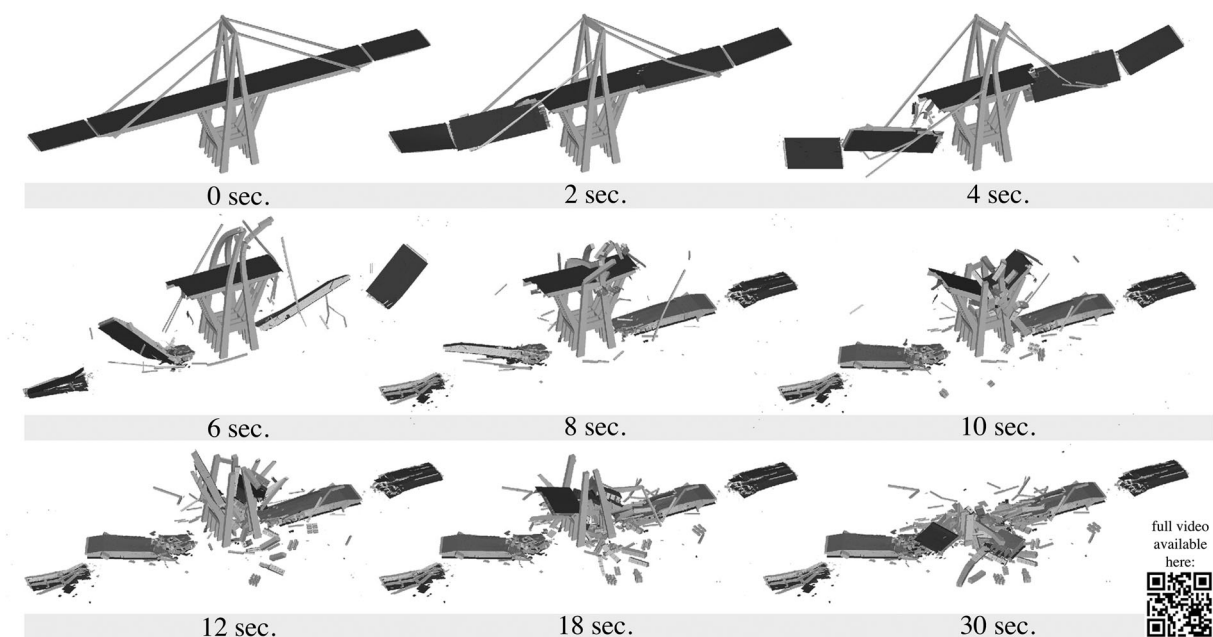


Fig. 19: Predicted collapse mechanism associated to a sudden failure of the connection between antenna and S-W stay

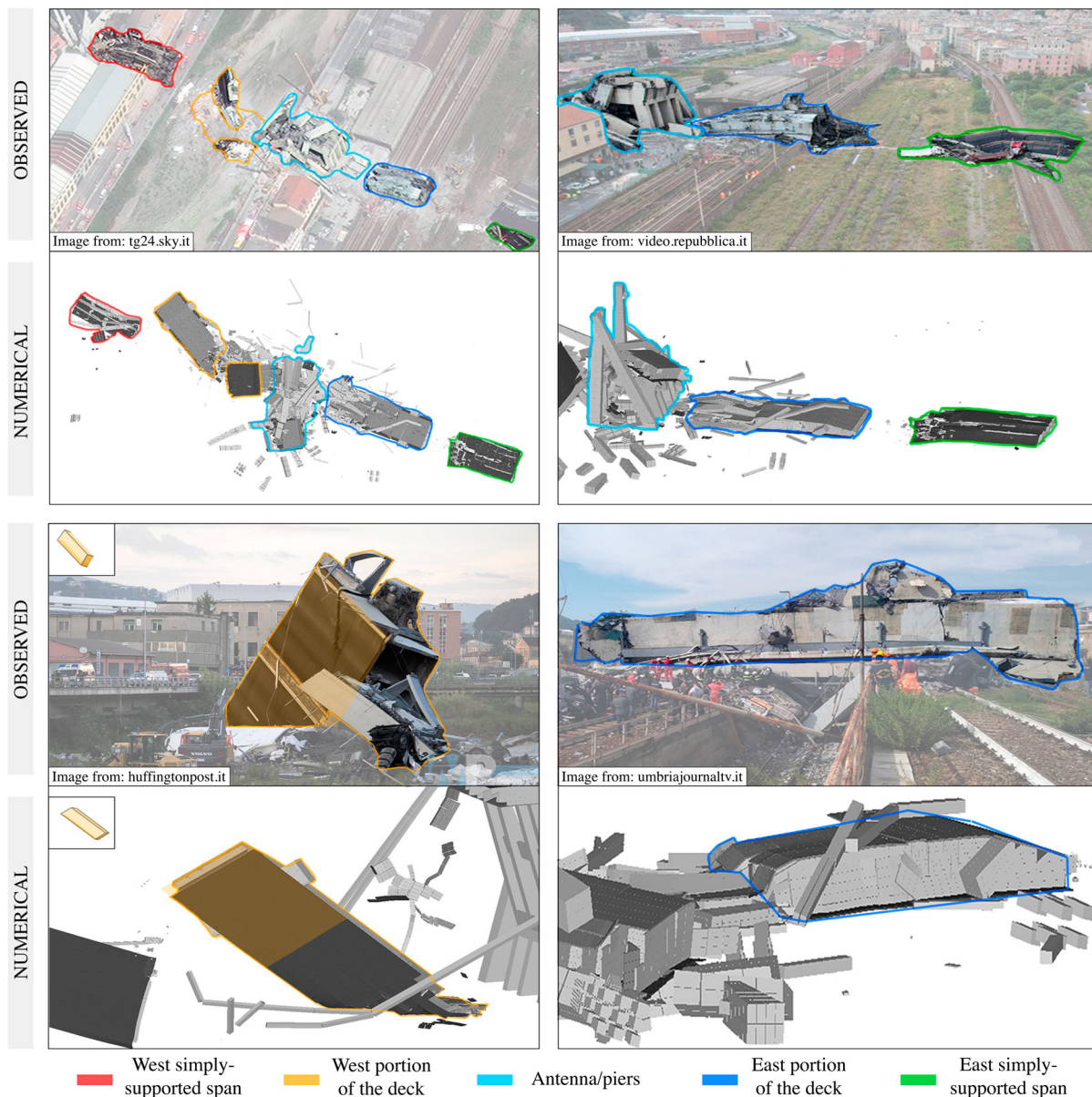


Fig. 20: Actual vs. predicted debris extent and configuration (identical colours are used to outline corresponding observed-modelled collapsed segments of the bridge)

## Concluding Remarks: What Might Have Happened

The introductory part of this paper tries to outline the exciting time of freeways booming construction in the 1950s and 1960s, with the rapid introduction of new, advanced construction technology and namely of large span pre-stressed bridge structures. In this daring context, the Morandi Bridge stands out as one of the most original and well-devised structures. However, it appears that some relevant aspects had not been properly considered, because of an insufficient level of knowledge, or because they were deliberately considered minor and not relevant, or simply because they were overlooked and taken for granted. Two typical examples are the long-

term effects of time dependent phenomena (such as creep and relaxation) and the actual injection of tendon ducts and the potential consequences in terms of corrosion; Morandi himself raised these issues in the year following the construction of the bridge.<sup>44</sup> With specific reference to the case under scrutiny, it appears that the tendon ducts were certainly poorly injected and possibly not injected at all in most cases, however, this regrettable situation does not appear to have had a serious impact on the collapse, unless in favouring the progression of corrosion.

In the main part of this study, well-known structural analysis codes were employed to model the structural system and equally well-established theories were used to calculate the

safety margins of different sections and elements. From these verifications, it can be concluded that:

- All elements, with no exception, had ample margins of safety towards failure, considering the structure as described at the time of construction.
- The addition of variable live loads seems to have little influence on the assessed demands, thus being an unlikely trigger of failure.
- An “exceptional” point load, acting on a critical section of the supported span may induce local element collapse, particularly in presence of relevant progress of corrosion.
- A local failure such as those mentioned in the previous point will not extend into a global collapse (e.g. a shear failure of at least two Gerber beams of the supported span may

induce the collapse of the span, but not bridge collapse).

- The progressive reduction of the steel section and the connected concrete compression in the stays would result in increased local displacements and significant deck level irregularities, long before a near collapse would have been reached.
- The structural over-strength is so relevant that the bridge is generally compliant with a seismic verification applying the actions considered today.
- The loss of a stay seems to be the final cause of collapse, regardless of the initiation of the collapse sequence.
- The possible initial cause of the collapse may thus be related to fatigue problems in the tendons near the tip of the antenna, or by deterioration of the connection between stay and transverse link. These local phenomena have not been explored, because of lack of detailed data.

As previously stated, all these considerations are based on elaborations of data publicly available; potential future cross-correlation with evidence of actual phenomena, such as corrosion or wires fracture, will allow a more thorough discussion of what really happened.

## Acknowledgements

The authors would like to acknowledge the valuable assistance of Maria Grazia Accurso-Tagano in the preparation of all the bridge drawings included in this paper. In addition, the authors are also grateful to Luis Alvarez, for his assistance in the moment-curvature analysis of the bridge deck. Finally, the assistance and collaboration of the technical support staff from Applied Science International LLC (ASI), on the use of the employed AEM software—Extreme Loading for Structures, is also greatly appreciated.

## ORCID

Gian Michele Calvi  <http://orcid.org/0000-0002-0998-8882>  
Gerard J. O'Reilly  <http://orcid.org/0000-0001-5497-030X>  
Nicola Scattarreggia  <http://orcid.org/0000-0002-3297-8068>  
Ricardo Monteiro  <http://orcid.org/0000-0002-2505-2996>  
Daniele Malomo  <http://orcid.org/0000-0002-4518-5841>  
Rui Pinho  <http://orcid.org/0000-0001-6767-9036>

## References

- [1] Petrovsky, H. *Engineers of Dreams: Great Bridge Builders and the Spanning of America*. New York: Alfred A. Knopf, Inc, 1995.
- [2] Weingroff, RF. The greatest decade 1956–1966 – Part 1: Essential to the national interest. *Public Roads (FHWA)*, March/April 2006.
- [3] Weingroff, RF. The greatest decade 1956–1966 – Part 2: The Battle of its life. *Public Roads (FHWA)*, May/June 2006.
- [4] Pérez-Peña, R. After Italy collapse, Europe asks: how safe are our bridges? *The New York Times*, 2018 Aug. 21.
- [5] Santarella, L, Miozzi E. *Ponti Italiani in Cemento Armato* (3rd ed.). Milan: Hoepli, 1948.
- [6] Stabilini, L. *Ponti* (III ed.). Libreria Editrice Politecnica Cesare Tamburini, Milan, 1950.
- [7] Iori, T, Poretti S. The golden age of “Italian style” engineering. Proceedings of the 3rd International Congress on Construction History, Cottbus, 2009.
- [8] Calvi, GM, Sullivan TJ, Villani A. Conceptual seismic design of cable-stayed bridges, *J, Earthquake Eng.* 2010; **14**(8):1139–1171.
- [9] Sozen, MA. *Structural Damage Caused by the Skopje Earthquake of 1963: A Report to the Committee on Masonry and Reinforced Concrete of the American Society of Civil Engineers and the American Concrete Institute*. Urbana: University of Illinois, 1964.
- [10] Gjorgjiev, I, Garevski M. Replacement of the old rubber bearings of the first isolated building in the world. Proceedings of the 15 WCEE, Lisbon, 2012.
- [11] Brocher, TM, Filson, JR, Fuis, GS, Haeussler, PJ, Holzer, TL, Plafker, G, Blair, JL. *The 1964 Great Alaska Earthquake and Tsunamis – A Modern Perspective and Enduring Legacies*. U.S. Geological Survey Fact Sheet 2014–3018, 2014. Available from: <https://dx.doi.org/10.3133/fs20143018>.
- [12] Corriere delle Alpi. *Capolavoro di ingegneria nel posto sbagliato*, 2013. Available from: <http://temi.repubblica.it/corrierealpi-diga-del-va-jont-1963-2013-il-cinquantenario/la-costruzione-della-diga/>.
- [13] OPCM 3274. Primi elementi in materia di criteri generali per la classificazione sismica del territorio nazionale e di normative tecniche per le costruzioni in zona sismica. G.U. of the Italian Republic, N. 108, 2003 May 8.
- [14] Von Kármán, T, Edson L. *The Wind and Beyond: Theodore von Kármán, Pioneer in Aviation and Pathfinder in Space*. Boston, MA: Little Brown, 1967.
- [15] Calvi, PM, Proestos GT, Ruggiero DM. Towards the development of direct crack-based assessment of structures. *ACI SP.* 2018; **328** (9):1–20.
- [16] Johnson, P M, Couture A, Nicolet R. *Report of the Commission of Inquiry into the Collapse of a Portion of the de la Concorde Overpass*. Gouvernement du Québec, 2007. ISBN 978-2-550-50961-5.
- [17] CBC News. Quebec to Destroy 28 Bridges, Repair Others. *CBC News Montreal*, 2008 Apr 9. Available from: <http://www.cbc.ca/news/canada/montreal/quebec-to-destroy-28-bridges-repair-others-1.710558>.
- [18] BBC News. Italian bridge collapses on busy road in Lecco. *BBC News Europe*, 2016 Oct 29. Available from: <http://www.bbc.com/news/world-europe-37810808>.
- [19] BBC News. Italy: Two die as motorway bridge collapses near Ancona. *BBC News Europe*, 2017 March 9. Available from: <http://www.bbc.com/news/world-europe-39218467>.
- [20] Fulloni, A. Crolla un viadotto a Fossano Schiacciata auto dei carabinieri. *Corriere della Sera*, 2017 April 18. Available from: [http://www.corriere.it/cronache/17\\_aprile\\_18/crolla-viadotto-fossano-schiacciata-auto-carabinieri-ae2f0300-243f-11e7-9ccc-1412672da04e.shtml](http://www.corriere.it/cronache/17_aprile_18/crolla-viadotto-fossano-schiacciata-auto-carabinieri-ae2f0300-243f-11e7-9ccc-1412672da04e.shtml).
- [21] Gazzetta del Sud. Edition of April 24, 1999.
- [22] Morandi, R. Il viadotto sul Polcevera per l'autostrada Genova-Savona. *L'Industria Italiana del Cemento*. 1967a; **XXXVII**:849–872.
- [23] Morandi, R. Il viadotto del Polcevera dell'Autostrada Genova – Savona. Roma, 1967b.
- [24] Morandi, B. La precompressione sistema Morandi M5. CESAP S.p.A, 1970.
- [25] DSI. DYWIDAG bonded post-tensioning systems using strands. Dywidag Systems International. Available from: <https://www.dywidag.com/fileadmin/downloads/dywidag-emea/dsi-dywidag-bonded-post-tensioning-systems-using-strands-eu.pdf>.
- [26] Mortellaro, AP, Ievoli G, Lombardo F, Nuti C, Vanzi I. *Relazione della Commissione Ispettiva Ministeriale crollo Viadotto Polcevera*. Roma: Ministero delle Infrastrutture e dei Trasporti, 2018.
- [27] Martinez y Cabrera, F, Camomilla G, Pisani F, Marioni A. Il risanamento degli stralli del viadotto Polcevera. *Atti delle Giornate AICAP*, 581–590, 1993.
- [28] Martinez y Cabrera, F, Camomilla G, Donferri Mitelli M, Pisani F. Rehabilitation of the stays of the Polcevera Viaduct. International Symposium on Cable Stayed Bridges, Shanghai, 640–665, 1994.
- [29] CSI. SAP2000 Integrated Software for Structural Analysis and Design, 2016. Available from: <https://www.csiamerica.com/products/sap2000>.
- [30] McKenna, F, Scott MH, Fenves GL. Nonlinear finite-element analysis software architecture using object composition. *J. Comput. Civ. Eng.* 2010; **24**(1):95–107.
- [31] NTC. Norme Tecniche per le costruzioni. Rome, 2008.
- [32] Bentz, EC. *Response-2000*, 2017. Available from: <http://www.ecf.utoronto.ca/~bentz/r2k.htm>.
- [33] Vecchio, FJ, Collins MP. The modified compression field theory for reinforced concrete elements subjected to shear. *ACI Journal*. 1986; **83**(2):219–231.
- [34] Rabbat, B, Collins, MP. A variable angle space truss model for structural concrete

- members subjected to complex loading. *ACI SP*. 1978; **55**: 547–587.
- [35] CSA. *Design of Concrete Structures*. A23.3-14. Mississauga: Canadian Standards Association, 2014.
- [36] Elshaer, A, Mostafa, H, Salem, H. Progressive collapse assessment of multistory reinforced concrete structures subjected to seismic actions. *KSCE J. Civ. Eng.* 2017; **21** (1):184–194.
- [37] Karbassi, A, Nollet, M-J. Performance-based seismic vulnerability evaluation of masonry buildings using applied element method in a nonlinear dynamic-based analytical procedure. *Earthq. Spectra*. 2013; **29** (2):399–426.
- [38] Malomo, D, Pinho, R, Penna, A. Using the applied element method to simulate the dynamic response of full-scale URM houses tested to collapse or near-collapse conditions. *16th European Conference on Earthquake Engineering, Thessaloniki, Greece*, 2018.
- [39] Salem, H, Mohssen, S, Nishikiori, Y, Hosoda, A. Numerical collapse analysis of Tsuyagawa Bridge Damaged by Tohoku tsunami. *J. Perform. Const. Facil.* 2016; **30** (6):04016065.
- [40] Meguro, K, Tagel-Din, H. Applied element method for structural analysis: Theory and application for linear materials. *Struct. Eng. Earthq. Eng.* 2000; **17**(1):21s–35s.
- [41] Meguro, K, Tagel-Din, H. Applied element simulation of RC structures under cyclic loading. *ASCE J. Struct. Eng.*. 2001; **127** (11):1295–1305.
- [42] Meguro, K, Tagel-Din, H. Applied element method used for large displacement structural analysis. *J. Nat. Dis. Sci.* 2002; **24**(1):25–34.
- [43] ASI (Applied Science International LLC). *Extreme Loading for Structures*. Durham (NC), 2018.
- [44] Morandi, R. The long-term behaviour of viaducts subjected to heavy traffic and situated in an aggressive environment: The viaduct on the Polcevera in Genoa. IABSE Reports of the Working Commissions, 032, 170–180, 1979.